Available online at www.CivileJournal.org

Civil Engineering Journal

(E-ISSN: 2476-3055; ISSN: 2676-6957)

Vol. 11, No. 12, December, 2025

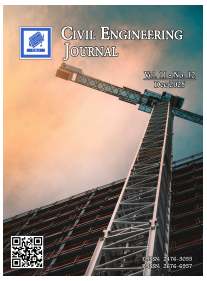

The Influence of Nanodiamonds and Aluminum Oxide Nanoparticles on the Structure and Properties of High-Strength Concrete

Alexey N. Beskopylny [1*], Yasin Onuralp Özkılıç [2, 3*], Sergey A. Stel'makh [2], Evgenii M. Shcherban' [4], Diana Elshaeva [2], Andrei Chernil'nik [2], Emrah Madenci [3, 5], Ceyhun Aksoylu [6]

[1] *Department of Transport Systems, Faculty of Roads and Transport Systems, Don State Technical University, 344003 Rostov-on-Don, Russia.*

[2] *Department of Unique Buildings and Constructions Engineering, Don State Technical University, 344003 Rostov-on-Don, Russia.*

[3] *Department of Civil Engineering, Faculty of Engineering, Necmettin Erbakan University, 42000 Konya, Turkey.*

[4] *Department of Engineering Geometry and Computer Graphics, Don State Technical University, 344003 Rostov-on-Don, Russia.*

[5] *Department of Technical Sciences, Western Caspian University, Baku, 1001, Azerbaijan.*

[6] *Department of Civil Engineering, Faculty of Engineering and Natural Sciences, Konya Technical University, 42075 Konya, Turkey.*

Received 20 June 2025; Revised 04 November 2025; Accepted 12 November 2025; Published 01 December 2025

Abstract

High-performance concrete (HPC) is an important construction material that can be improved with nano-additives. In this study, the modification of HPC with KHA-HC nanodiamond and nano aluminum oxide (NA) admixtures was investigated; the admixture rate was applied in the range of 0-1.4% in 0.2% increments. The rheology, density, compressive and flexural strength, water absorption, and microstructure properties were investigated; the results showed that the KHA-HC nanodiamond showed higher efficiency than NA. Compared with HPC without nano-additives, the strength properties of HPC with the most optimal content of nano-additives, 0.6% KHA-HC and 1.0% NA, were improved by 47.1% and 17.0% for compressive strength and by 44.9% and 16.3% for flexural strength. Water absorption decreased by 33.0% and 26.0%, respectively. Also, with optimal dosages of nano-additives, an improvement in the rheology of the HPC mixture was recorded. The complex modification of HPC 0.6% KHA-HC and 1.0% NA provides a synergistic effect and maximum improvements in properties: the increase in compressive strength was 58.2%; flexural strength - 54.1%; decrease in water absorption - 49.1%. HPC modified by nano-additives has an improved macro- and microstructure. The two types of nano-additives' effectiveness, KHA-HC and NA, both separately and together in HPC technology for additional improvement of their operational properties, has been proven.

Keywords: High-Performance Concrete; Nano-Additives; Nanodiamonds; Nano-Sized Aluminum Oxide; Nanoparticles.

1. Introduction

High-performance concrete (HPC) is a special cement-based concrete that can reach a compressive strength of over 50 MPa and is distinguished by its superior durability properties [1, 2]. HPC, which plays an important role in sustainable building production, has been intensively investigated in the field of building materials science in recent years [3-6]. The performance of this concrete is highly dependent on the mix design. The standard HPC composition includes a mixture of cement, fine aggregate, and various types of fillers, such as microsilica, fly ash, quartz powder, and others.

* Corresponding author: besk-an@yandex.ru; yozkilic@erbakan.edu.tr

http://dx.doi.org/10.28991/CEJ-2025-011-12-08

The optimal combination of a binder, fine aggregate, and fillers in combination with plasticizing additives allows achieving the densest packing of particles, which ensures the high strength properties of HPC [7-10]. The use of new types of admixtures is one of the most effective mix design approaches to improve the performance of concrete in both normal concrete and high-performance concrete technology [11, 12]. For example, the inclusion of additional pozzolanic materials such as calcined kaolin clay and nanolime in self-compacting high-strength concrete allows for significant improvements in compressive and tensile strength properties during splitting [13]. Selecting the optimal maximum size of coarse aggregate allows for an increase in the strength properties of HPC [14]. Optimal selection and combination of recycled aggregates allow for the production of high-strength concrete with improved mechanical properties [15].

Among the numerous additives, nanomaterials with unique physical and chemical properties are of particular interest [16]. Including nanomaterials in concrete composites offers a new approach to improving their properties. A new theoretical field of knowledge is also being formed aimed at studying and understanding the mechanisms of interaction of nanomaterials with other components of cement composites, and an applied research area focusing on identifying the most suitable types and utilization rates of nanomaterials to improve concrete performance is rapidly developing [17, 18]. Among the various nanomaterials, the most popular modifying additives in concrete technology are nanosilica (NS) and nano calcium carbonate (NC). For example, the inclusion of 2% colloidal NS accelerates the process of hydration reactions and increases strength by 22.2% [19]. The use of 2% nanosilica (NS) as a secondary filler significantly improves the sulfate resistance of concrete, while reducing chloride permeation by about 30% and increasing compressive strength by up to 15% [20]. NS also improves the impermeability of concrete and increases its resistance to chloride ions [21]. The addition of nanosilica to cement mortar has been found to increase the self-healing capacity of the material [22]. High-performance concrete modified with NS demonstrates improved microporous structure and higher strength properties [23, 24]. Also, the use of nanosilica (NS) in ultra-high-performance concrete strengthens the material's resistance to corrosion [25].

Various studies have shown that the addition of nanosilica (NS) to concrete mixtures significantly increases the mechanical strength and durability of the material [26-29]. Adding 1% nano-calcium carbonate ($CaCO_3$) to concrete strengthens the microstructure of the material, reduces permeability and increases mechanical strength [30, 31]. High-strength concrete on recycled aggregate modified with 2.5% NC has higher compressive strength and ductility [32]. Several studies have reported that modifying high-strength concrete with appropriate amounts of nano-calcium carbonate ($CaCO_3$) increases both its mechanical strength and durability [33–35]. In addition to the above-mentioned types of additives based on NS and NC nanoparticles, an additive based on aluminum oxide (NA) nanoparticles is also used in cement composite technologies. However, it should be noted that the use of NA in modifying conventional and high-strength concrete has not been as widely studied in comparison with such additives based on nanomaterials as NS and NC [36]. For example, the addition of nano-aluminum oxide (Al_2O_3) to foam concrete mixes strengthened foam stability and resulted in an increase in compressive strength of up to 79% [37]. Adding up to 1% nano-aluminum oxide (NA) to ultra high-performance concrete improves both the workability of the mix and its mechanical strength and microstructure [38]. Introducing 2% NA with 1.5% glass fiber into the composition of self-compacting concrete provided an increase in compressive strength by 61% and tensile strength by 107.6% [39].

Ahmed & Alkhafaji [40] also proves the possibility of improving the strength properties and wear resistance of concrete by modification with NA particles. Nanodiamonds are carbon nanostructures with a diamond-type crystal lattice, where the size of one crystal varies from 1 nm to 10 nm [41]. Currently, the possibility of using nanodiamonds as an active and modifying component is actively studied in various industries, such as medicine, bioengineering, coating technologies and lubricating fluids [42-45]. Nanodiamonds have been effectively used in the formulation of multifunctional carbon nanocomposite hydrogels for wound healing [46]. Carbon coatings based on nanodiamonds can reduce the friction coefficient and wear rate of moving parts of mechanical systems [47]. It has been proven that enrichment of lubricating compositions with nanodiamonds improves their tribological properties [48]. Within the scope of building materials science, it is noteworthy that studies on the use of nanodiamonds as modifier additives in cement composites are very limited [49]. The possibility of using chemically pure nanodiamonds of cavitation synthesis as a modifying additive for concrete was previously proven. Introducing nanodiamonds into the composition of concrete allows increasing the intensity of strength gain and improving its mechanical properties [50]. The positive effect of modification with nanodiamonds on cement composites has also been proven in several other studies [51, 52]. In general, speaking about carbon nanomaterials, the possibility of their use as modifying additives in cement concrete technology is confirmed by scientific research. Including up to 0.1% of multilayer carbon nanotubes in the composition of concrete allows reducing its porosity and increasing resistance to sulfate corrosion [53]. Optimization of the concrete composition with carbon nanotubes in the optimal amount allows to increase the concrete strength in bending and compression and to reduce the carbonation depth by 26.9% [54]. Similarly, in other works, including the optimal amount of carbon nanotubes in the composition of cement concretes allowed for the improvement of their mechanical and operational properties [55-59].

Introducing nanomaterials in the technology of manufacturing modern building materials, in particular in high-performance concrete, is a promising direction and is highly relevant. In the study, aluminum oxide nanoparticles (NA)

and pure nanodiamonds obtained by the cavitation method (KHA-HC) were preferred as nanoadditives. The combined use of the additives discussed in this study in high-strength concrete and their comparison with other complex nanoadditives has not previously been reported in the literature. The scientific novelty of this study is the development of new high-performance concrete mixtures modified with aluminum oxide nanoparticles and pure nanodiamonds obtained by cavitation method and the demonstration of new relationships between the properties and microstructure of HPC and the modification parameters when these admixtures are used alone or in combination. The aim of this study was to determine the optimum parameters for modifying high performance concrete with aluminum oxide (NA) and cavitation synthesized pure nanodiamonds (KHA-HC) admixtures and to investigate the effects of these nano-additives on the mechanical, physical properties and microstructure of HPC. The objectives of the work included:

- Developing experimental design of HPC blends considering raw material properties and determination of optimum ranges (minimum and maximum values) where modification with nano additives can be applied;
- Producing experimental HPC samples modified with nanoadditives in various dosages;
- Conducting a series of laboratory studies to evaluate the workability parameter of mixture properties, density, compressive and flexural strengths and water absorption capacities of HPC specimens obtained from the control composition and with different NA and KHA-HC content;
- Studying the structure of HPC modified with nanoadditives using scanning electron and optical microscopy;
- Processing experimental data and determining the optimal dosages of NA and KHA-HC in HPC.

This study has the following structure. Section 1 presents the relevance of the study, the literature review, and scientific novelty. It also presents the purpose and tasks of the study. Section 2 presents the materials and methods of the study. Section 3 presents the results of the experimental studies and their analysis. Section 4 contains the conclusions. Section 5 presents the Author Contributions, Data Availability Statement, Funding, Acknowledgements, and Conflicts of Interest. Section 6 contains a numbered list of references.

2. Materials and Methods

2.1. Materials

The raw materials selected for the production of HPC included: Portland cement CEM I 52.5 N (NOVOROSCEMENT, Novorossiysk, Russia); quartz sand (Nedra, Samarskoye, Russia); quartz filler (ROSKARB, Novokaolinovy, Russia); microsilica (NLMK, Lipetsk, Russia); hyperplasticizer Sika ViscoCrete-200 (SIKA AG, Baar, Switzerland). The properties and chemical compositions of the basic raw materials used in the study are shown in detail in Tables 1 to 5.

Table 1. Properties of Portland cement CEM I 52.5 N (PC)

Title					Actual value			
Specific surface area according to Blaine (cm²/g)					3300			
Setting time:								
Start (min.)					180			
End (min.)					270			
Uniformity of volume change (mm)					0.5			
Normal density (%)					29.3			
Compressive strength at the age of 28 days (MPa)					63.0			
Bending strength at the age of 28 days (MPa)					8.6			
Chemical Composition								
SiO_2 (%)	**Al_2O_3 (%)**	**Fe_2O_3 (%)**	**CaO (%)**	**MgO (%)**	**(Na_2O+0.658 K_2O) (%)**	**SO_3 (%)**	**Chlorine ion Cl (%)**	**LOI (%)**
19.15	5.27	4.80	65.17	1.16	0.50	3.00	0.008	0.94

Table 2. Properties of quartz sand (QS)

Title	Actual value
Bulk density (kg/m³)	1350
Apparent density (kg/m³)	2598
The content of dust and clay particles (%)	0.07
Content of clay in lumps (%)	0
Fineness modulus	1.79

Table 3. Properties of quartz filler (QF)

Title	Actual value
Mass fraction of calcium carbonate ($CaCO_3$) (%)	98.5
pH value	9.5
Moisture (%)	0.13
Bulk density (g/cm^3)	1.15

Table 4. Properties of microsilica (MS)

Title					Actual value				
Bulk density (kg/m^3)					153				
Chemical Composition									
SiO_2 (%)	Al_2O_3 (%)	Fe_2O_3 (%)	CaO (%)	MgO (%)	Na_2O (%)	K_2O (%)	C (%)	S (%)	LOI (%)
92.1	0.66	0.85	1.5	1.03	0.61	1.23	0.94	0.27	0.81

Table 5. Properties of hyperplasticizer Sika ViscoCrete-200 (SV)

Title	Actual value
Density (kg/dm^3)	1.06
pH value	6.0

The grain size distribution of sand, cement, quartz filler and microsilica particles is presented in Figure 1.

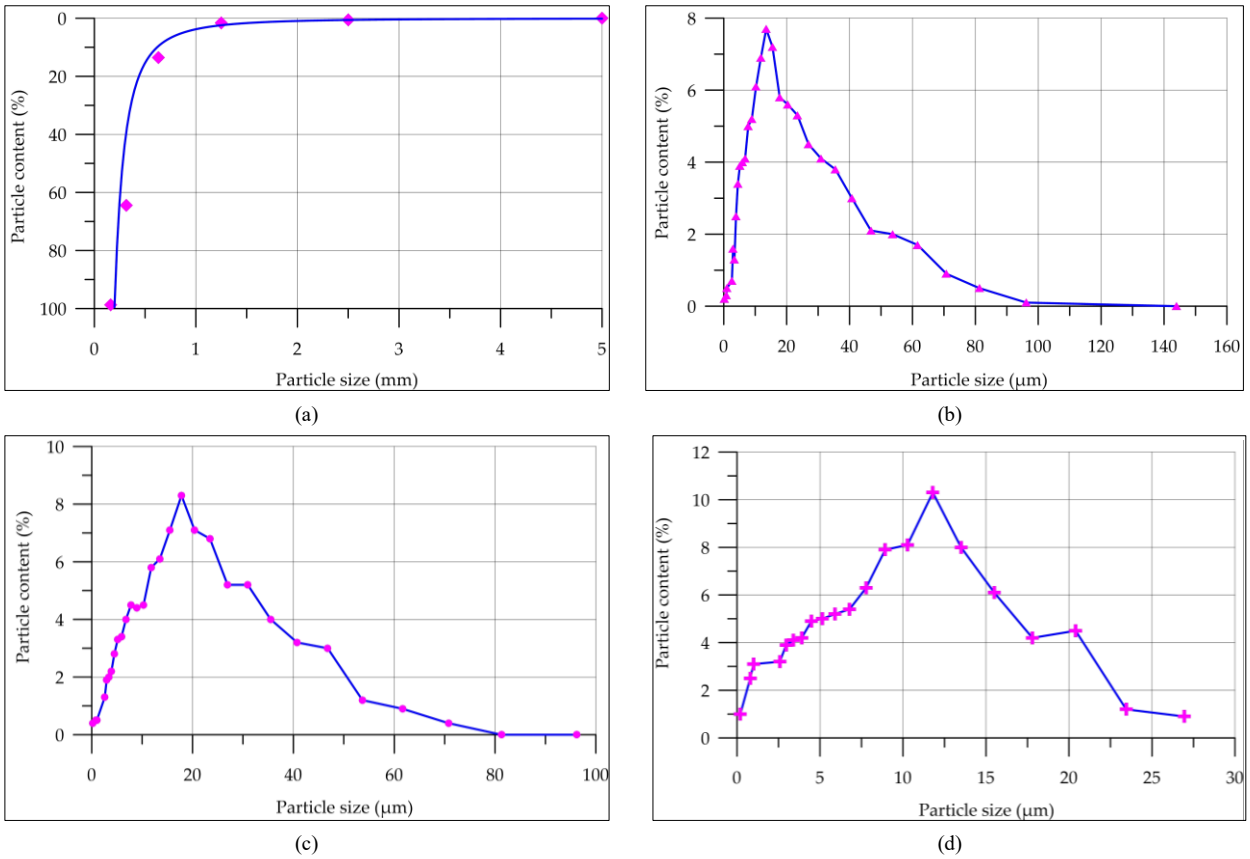

Figure 1. Particle size distribution curves: (a) QS; (b) PC; (c) QF; (d) MS

According to Figure 1-a, the total residues on sieves with numbers 5, 2.5, 1.25, 0.63, 0.315, and 0.16 were 0%, 0.6%, 1.6%, 13.5%, 64.5%, and 98.7%, respectively. The largest share of cement particles (Figure 1-b) 94.1% is in the size range from 3 to 31 μm, quartz filler particles (Figure 1-c) in the main share 86.7% are distributed in the size range from 3 to 35 μm, microsilica particles (Figure 1-d) have the following distribution pattern: 31.9% of particles are up to 5 μm in size and 66% in the range from 5 to 21 μm. Two types of modifying nanoadditives were used: chemically pure nanodiamonds of cavitation synthesis (KHA-HC) (Nanosystems, Rostov-on-Don, Russia) and nanosized aluminum

oxide (NA) (Lonwin Chemical Industry Group, Shanghai, China). Pure nanodiamonds produced by cavitation are sp^3 hybridized carbon nanoparticles with diamond-like structure and particle sizes limited to less than 3 nm in cross section. A detailed analysis illustrating the size and shape of nanodiamond particles is presented in an earlier study [50]. The colloidal solution of KHA-HC nanodiamonds shows no sedimentation over a period exceeding 1.5 years [50]. Figure 2 shows the results of TEM analysis (transmission electron microscopy) of KHA-HC particles.

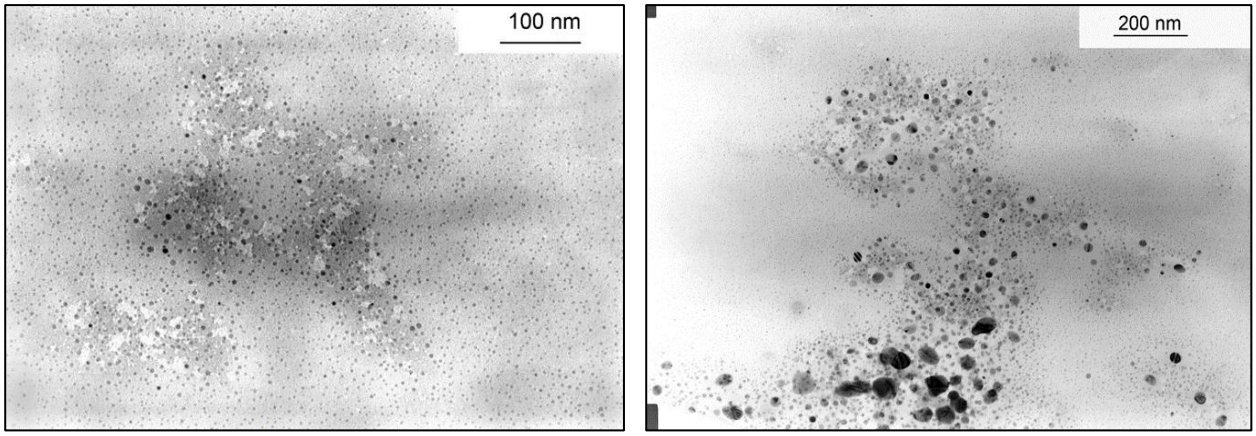

(a) (b)

Figure 2. Results of TEM analysis of synthesized nanodiamonds: (a) 100 nm; (b) 200 nm

Nanodiamond particles have a spheroidal shape and uniform distribution throughout the volume, indicating a high degree of hydration. NA is a white powder in the size range of 100-200 nm. Figures 3 and 4 show the results of SEM (Figure 3) and EDS analysis (Figure 4) of NA particles.

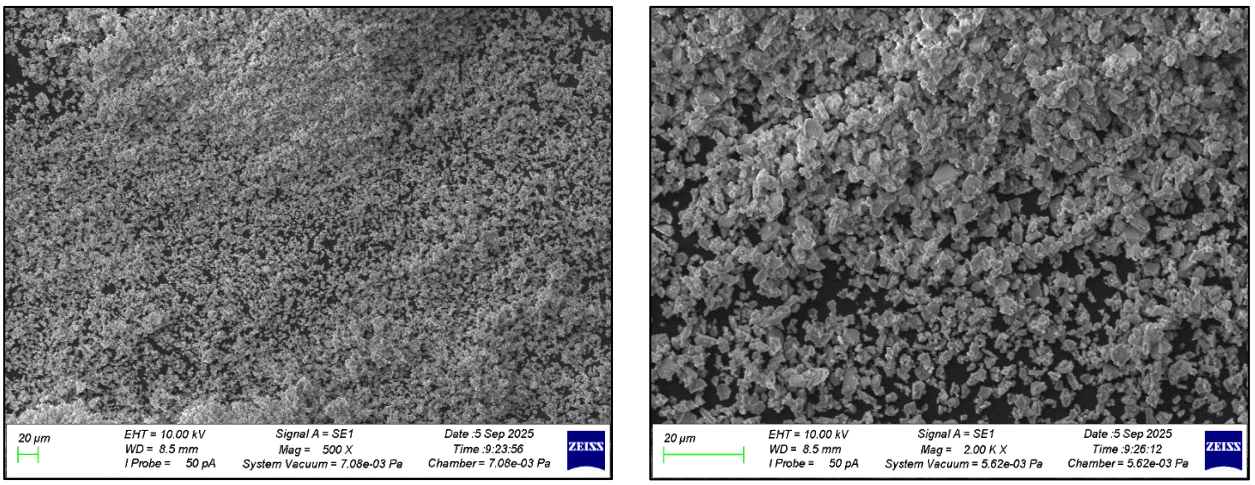

(a) (b)

Figure 3. SEM image of NA: (a) at 500X magnification; (b) at 2000X magnification

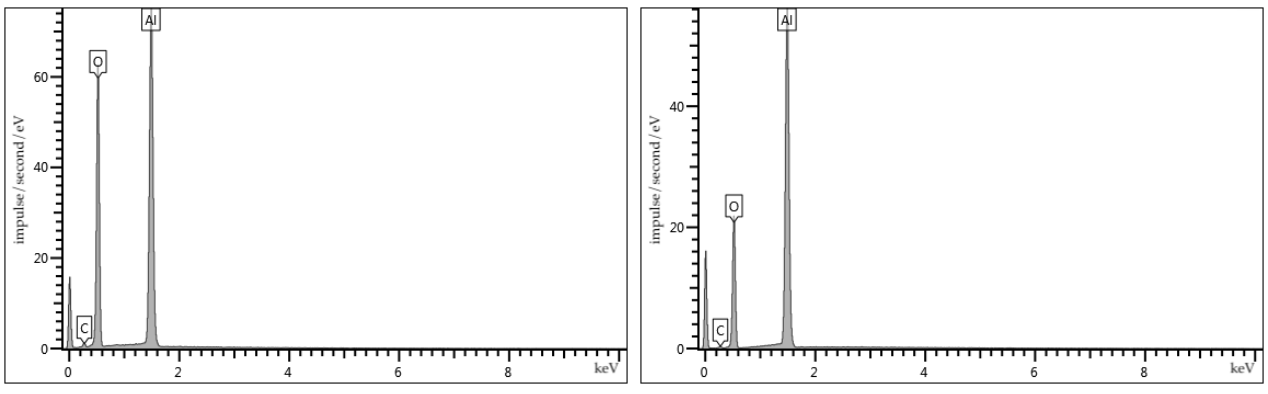

(a) (b)

Figure 4. EDS analysis of NA particles: (a) spectrum 1; (b) spectrum 2

Based on the results of EDS analysis of NA particles, the following chemical elements were identified: Al, O, C. The predominant elements are Al and O. The Al content in the 1st and 2nd spectra was 51.84% and 67.48%, respectively. The O content in the 1st and 2nd spectra was 46.28% and 31.55%, respectively. A small amount of C was recorded, which in the 1st and 2nd spectra was 1.88% and 0.96%, respectively.

The appearance of the modifying additives is shown in Figure 5.

(a) KHA-HC nanodiamonds colloidal solution (stable >1.5 years)

(b) NA white powder with particle size 20–100 nm.

Figure 5. Appearance of nanoadditives: KHA-HC; NA

2.2. Methods

The composition of HPC mixtures modified with different amounts of nanoadditives are presented in Table 6. The effects of nano-additives on HPC were investigated in comparison with a control mixture without nano-additives. The HPC blends were modified using KHA-HC and NA nano-additives in the range of 0-1.4% with an increase of 0.2% at each step.

Table 6. HPC compositions with nanoadditives

Mixture type	PC (kg)	QS (kg)	QF (kg)	MS (kg)	SV (kg)	KHA-HC (L/%)	NA (kg/%)	Water (L)
Control composition	760	835	370	38	41.8	–	–	210
KHA-HC/0.2	760	835	370	38	41.8	1.5/0.2	–	210
KHA-HC/0.4	760	835	370	38	41.8	3.0/0.4	–	210
KHA-HC/0.6	760	835	370	38	41.8	4.6/0.6	–	210
KHA-HC/0.8	760	835	370	38	41.8	6.1/0.8	–	210
KHA-HC/1.0	760	835	370	38	41.8	7.6/1.0	–	210
KHA-HC/1.2	760	835	370	38	41.8	9.1/1.2	–	210
KHA-HC/1.4	760	835	370	38	41.8	10.6/1.4	–	210
NA/0.2	760	835	370	38	41.8	–	1.5/0.2	210
NA/0.4	760	835	370	38	41.8	–	3.0/0.4	210
NA/0.6	760	835	370	38	41.8	–	4.6/0.6	210
NA/0.8	760	835	370	38	41.8	–	6.1/0.8	210
NA/1.0	760	835	370	38	41.8	–	7.6/1.0	210
NA/1.2	760	835	370	38	41.8	–	9.1/1.2	210
NA/1.4	760	835	370	38	41.8	–	10.6/1.4	210
KHA-HC/0.6+ NA/1.0	760	835	370	38	41.8	4.6/0.6	7.6/1.0	210

The selected dosage range (0-1.4% in 0.2% increments) was determined to be the most optimal based on the results of preliminary pilot experiments. The results also confirm that the effectiveness of the nanoadditive begins to decline at 0.8% for KNA-NS and at 1.2% for NA. Therefore, increasing the dosage range for additives beyond 1.4% is not advisable in the context of this study.

The technology for preparing the control HPC mixture and manufacturing samples included the following stages:

Stage 1. Dosing dry concrete components, SV and water in the required quantity.

Stage 2. Mixing SV and water.

Stage 3. Loading PC and QS into the mixer and mixing them dry for 30 seconds.

Stage 4. Adding QF and MS to the dry mixture of cement and sand and mixing for 30 seconds.

Stage 5. Adding water and additives to the dry mixture of raw components and mixing until a homogeneous mixture is obtained.

Stage 6. Pouring the HPC mixture into molds and vibration molding.

Stage 7. Removing HPC samples from the molds after 24 hours and keeping them for 28 days in a normal curing chamber at a temperature of (20±2) C and a relative air humidity of (95±5)%.

The preparation of HPC blends with KHA-HC additives followed the same procedure in general, but different applications were performed in Stage 2 and Stage 5. At stage 2, the mixing water was divided into two parts. One part of the water was mixed with SV, the other part with KHA-HC. At stage 5, the water with additives was introduced in stages: first, water with SV was poured in, then water with KHA-HC. The preparation of HPC mixtures with the NA additive was also carried out in a similar manner as in the case of the control mixture with a difference at stage 4. After introducing PC + QS into the dry mixture, QF and MS were added with further mixing for 30 secondsThen, the NA additive was added to the dry ingredients mixture and mixed homogeneously for 60 seconds. The preparation of the HPC mixture with the KHA-HC and NA nanoadditive complex was carried out taking into account the above-described features at stages 2, 4 and 5.

The accepted differences in the technology for preparing HPC mixtures are necessary for the best distribution of additives in HPC mixtures and are justified by the different aggregate states of the substances. The experimental study scheme, reflecting the total number of manufactured experimental HPC compositions, dosages of nanoadditives, types of experimental studies performed and the number of samples, is shown in Figure 6.

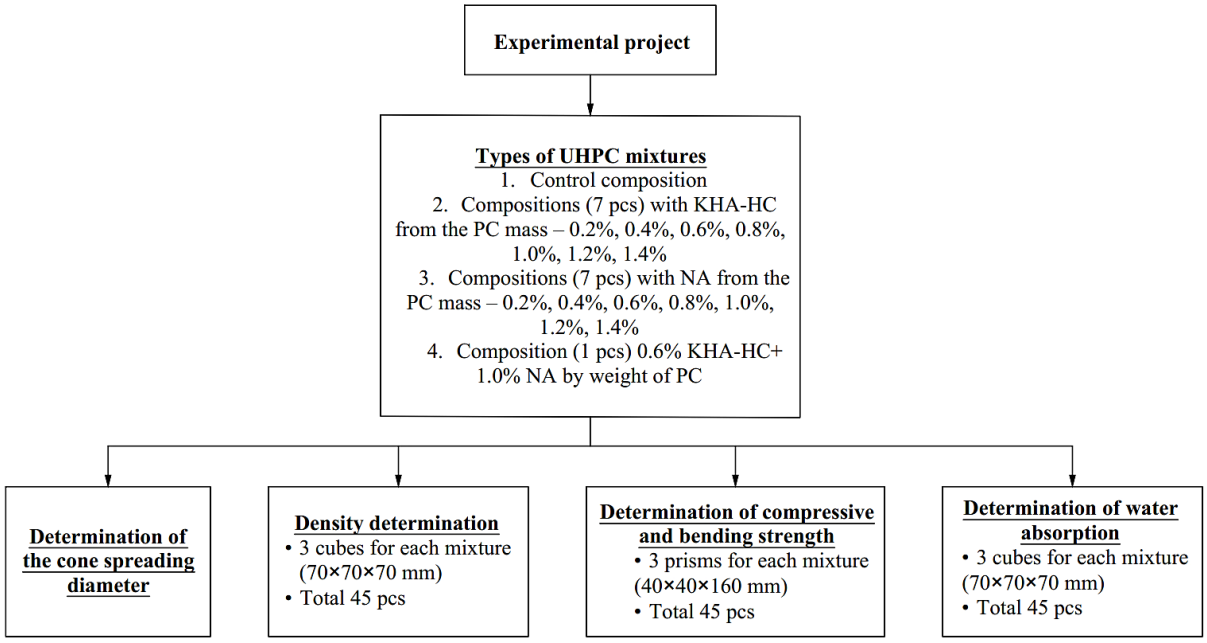

Figure 6. Experimental study scheme

The workability properties of HPC were measured using the cone spread index (slump flow) in accordance with the relevant standard [60]. Before starting the experiment, the base plate was placed on a flat and horizontal surface and the surface was cleaned with a damp cloth. The cone was placed in the center of the base plate. The cone was then filled with the mixture for 30 seconds, and any excess was removed. The cone was lifted in one movement for 1-3 seconds without interfering with the spread of the mixture. After the mixture stabilized, the widest spreading diameter (*d1*) was measured, then the diameter of this spreading in the direction perpendicular to d1 (*d2*) was determined and signs of segregation of the mixture were observed. The difference between d_1 and d_2 should not exceed 5 cm. The average cone spread value (CSD) is calculated using Equation 1:

$$CSD = \frac{(d_1 - d_2)}{2} \quad (1)$$

where, d_1 is the largest diameter of spreading flow (cm); d_2 is spreading flow at an angle of 90° to d_1 (cm).

The density, compressive strength, bending strength and water absorption of the experimental HPC compositions were determined at the age of 28 days. Density values of HPC samples were measured using methods in accordance with the relevant standard [61]. Before testing, the HPC samples were dried until they reached a constant mass. The volume of the samples was determined by measuring the geometric dimensions with a ruler. The average density of concrete was calculated using the formula:

$$\rho = \frac{m}{V} \times 1000 \quad (2)$$

where, m is the sample mass (g); V is the sample volume (cm^3).

The compressive and flexural strengths of the high-performance composites were measured according to the methods described in reference [62]. Prior to testing, HPC specimens were visually inspected for defects and geometric measurements were taken. The specimens were placed in a special laboratory setup and loaded with a load increase rate of 0.05 ± 0.01 MPa/s. Halves of the prism-shaped specimens were placed on special compression plates and subjected to compressive tests with a load increase rate of 0.6 ± 0.2 MPa/s. Compressive and flexural strengths were calculated using Equations 3 and 4:

$$R = \frac{F}{S} \quad (3)$$

where, F is the breaking load (N); S is the working cross-sectional area of the sample (mm^2):

$$R_{tb} = 1.5\frac{Fl}{b^3} \quad (4)$$

here l=100 mm, b=40 mm.

The appearance of experimental HPC samples modified with different types of nanoadditives and the process of determining their strength properties are shown in Figure 7.

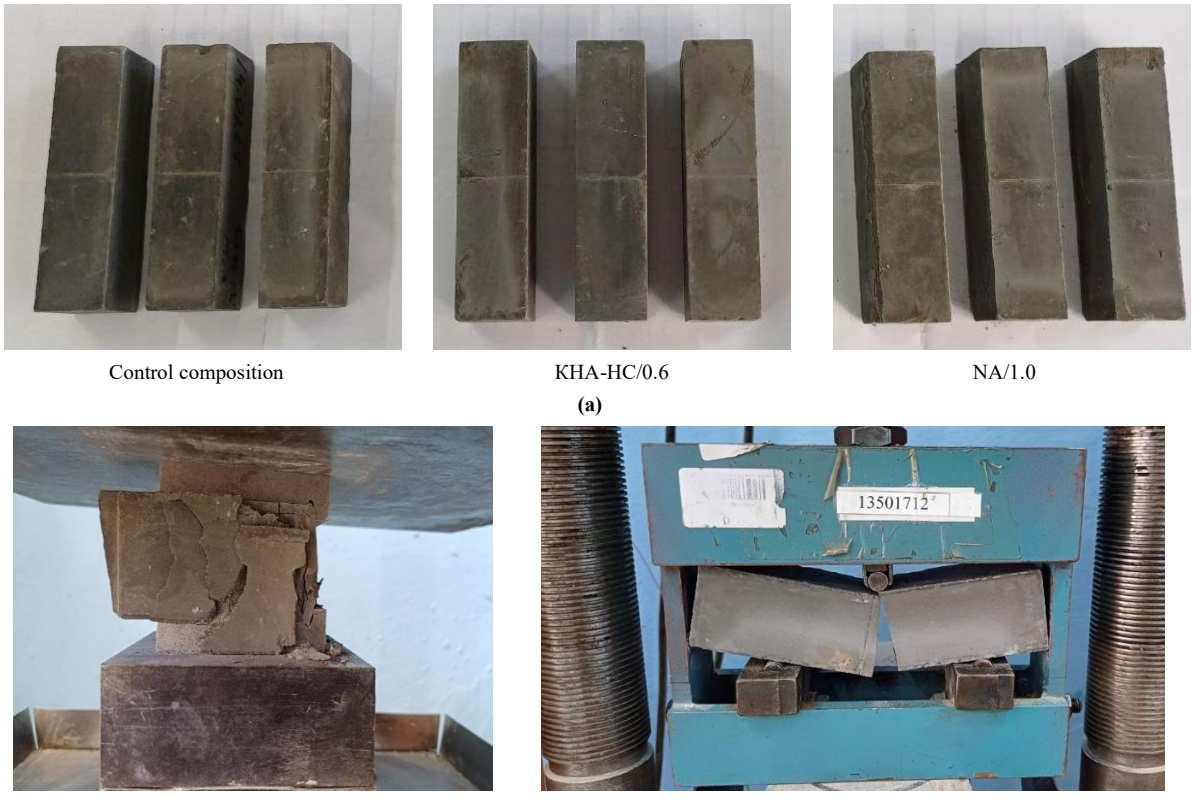

Figure 7. Experimental HPC samples: (a) appearance; (b) in the compressive strength test; (c) in the flexural strength test

The water absorption capacity of HPC samples was measured in accordance with the relevant standards and methods. [63, 64]. HPC samples dried to constant weight were placed in a container of water and allowed to saturate for 24 hours and then weighed. The saturation process was repeated until the difference between the last two measurements did not exceed 0.1%. The water absorption rate was calculated using the relevant formula:

$$W = \frac{m_w - m_d}{m_d} \times 100 \quad (5)$$

where, m_w is the mass of the water-saturated sample (g); m_d is the mass of the dry sample (g).

To evaluate the surface morphology and analyze the elemental composition, scanning electron microscopy studies were carried out using a Zeiss EVO MA 18 general-purpose scanning electron microscope (SEM) (Carl Zeiss Industrielle Messtechnik GmbH, Oberkochen, Germany) equipped with an X-Max 50N energy-dispersive spectrometer (EDS) (Oxford Instruments, Abingdon, England) built into the electron microscope.

3. Results and Discussion

The results of cone spread size distribution (CSD) determination of HPC mixtures modified with KHA-HC and NA additives are shown in Figure 8.

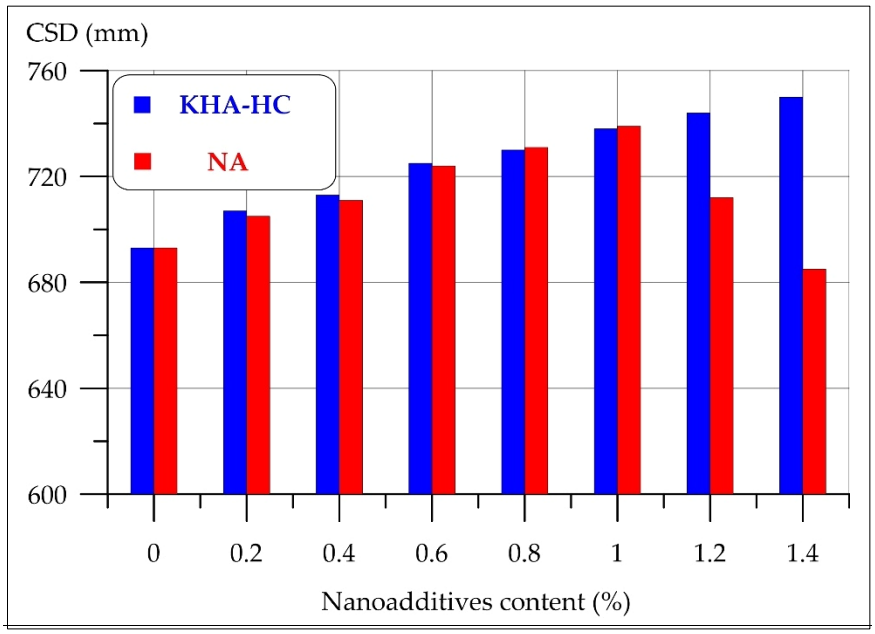

Figure 8. Dependence of the cone spread (CSD) of HPC mixtures on the content of KHA-HC and NA

According to the cone spread test results of HPC blends with KHA-HC additives shown in Figure 8, the workability (cone spread value) of the blend increases with increasing KHA-HC content. The maximum cone spread value of 750 mm was recorded for the KHA-HC/1.4 type composition, which is 8.2% higher compared to the cone spread value of the control mixture. The increase in the cone spread of HPC mixtures modified with KHA-HC in the range from 0.2% to 1.4% is primarily explained by the aggregate state of the additive, which is a colloidal solution of nanodiamonds [50, 51]. The dependence of the cone spread of HPC mixtures modified with NA had a slightly different character. The introduction of NA in the amount from 0.2% to 1.0% led to an increase in flow. The highest flow value of 739 mm was demonstrated by the NA/1.0 mixture, which is 6.6% higher than the control. A higher content of NA particles of 1.2% and 1.4% had the opposite effect, and the flow values of the mixture decreased to 712 mm and 685 mm, respectively. The inclusion of aluminum oxide nanoparticles up to 1% improves workability. NA particles at an optimal dosage fill the voids between other raw materials inside the HPC mixture. Filling the pores and voids with NA particles reduces the need for water and displaces it. Water displaced from the pores and voids contributes to an increase in the workability of HPC mixtures. However, at higher dosages, NA particles begin to agglomerate, which leads to their poor dispersion in HPC mixtures and, as a consequence, to a decrease in the cone spread values [38, 65]. The ΔCSD values, showing the changes in the cone spread of HPC mixtures depending on the type and amount of nanoadditives, are presented in Table 7.

Table 7. Change in HPC cone spread depending on the KHA-HC and NA amount

Nanoadditives Type	Nanoadditives content (%)							
	0	0.2	0.4	0.6	0.8	1.0	1.2	1.4
	ΔCSD (%)							
KHA-HC	0	2.0	2.9	4.6	5.3	6.5	7.4	8.2
NA	0	1.7	2.6	4.5	5.5	6.6	2.7	–1.2

Density (ρ) values of HPC samples modified with KHA-HC and NA additives are shown in Figure 9.

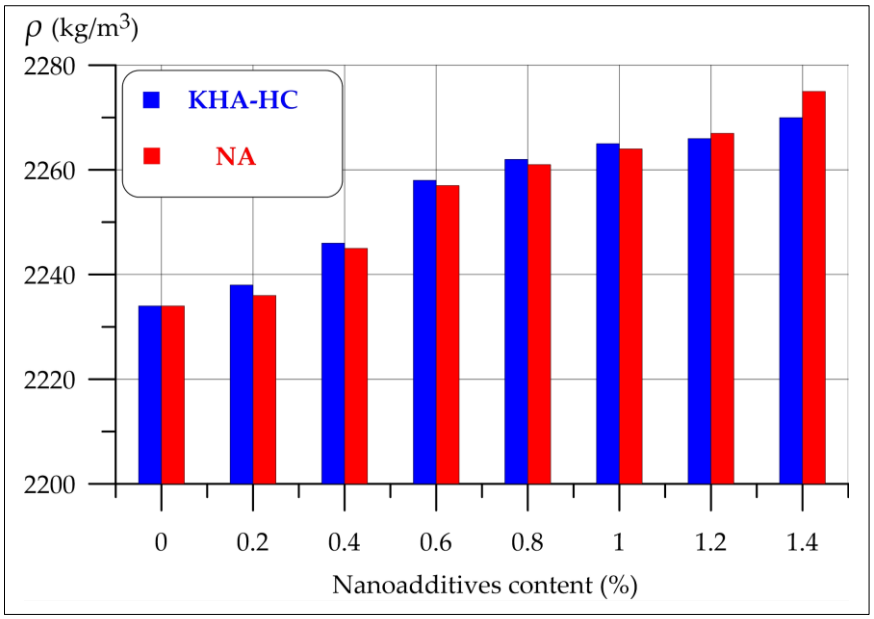

Figure 9. Dependence of the density (ρ) of HPC on the content of KHA-HC and NA

According to Figure 9, the density of HPC modified with KHA-HC in amounts from 0.2% to 1.4% varied from 2238 kg/m^3 to 2270 kg/m^3. The density of HPC modified with NA in amounts from 0.2% to 1.4% varied from 2236 kg/m^3 to 2275 kg/m^3. The addition of the specified amounts of nano additives to the HPC mixtures did not significantly change the density values of the samples. When the amount of nano-additives was increased, a slight increase in density was recorded; at a maximum additive level of 1.4%, the density of KHA-HC admixed concrete increased by 1.6% and that of NA admixed concrete by 1.8%.

Furthermore, Figures 10 and 11 present the strength test results of KHA-HC and NA doped HPC specimens. Figure 10 graphically shows the variation of the compressive strength (R_b) of HPC with respect to the amount of KHA-HC and NA additives.

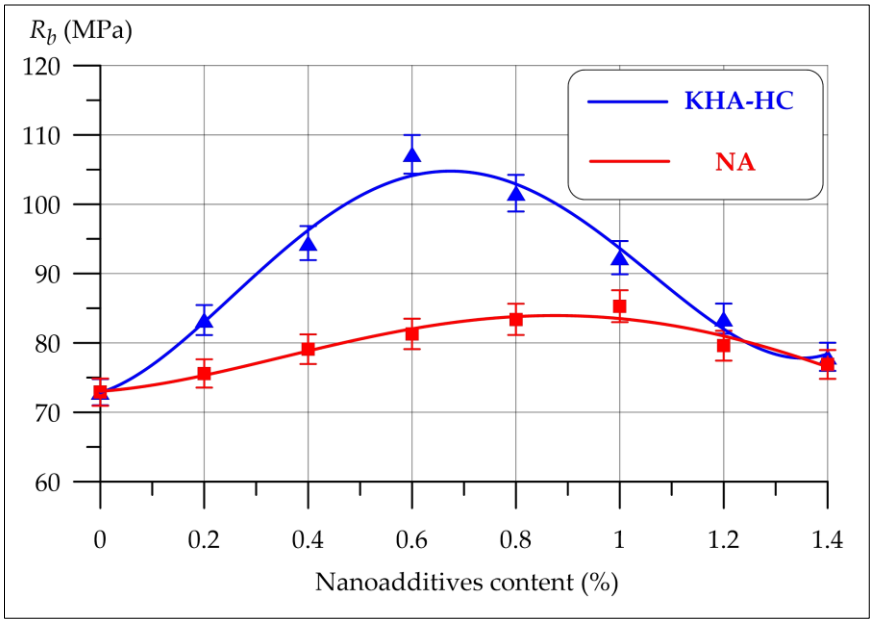

Figure 10. Compressive strength (R_b) of HPC versus KHA-HC and NA content

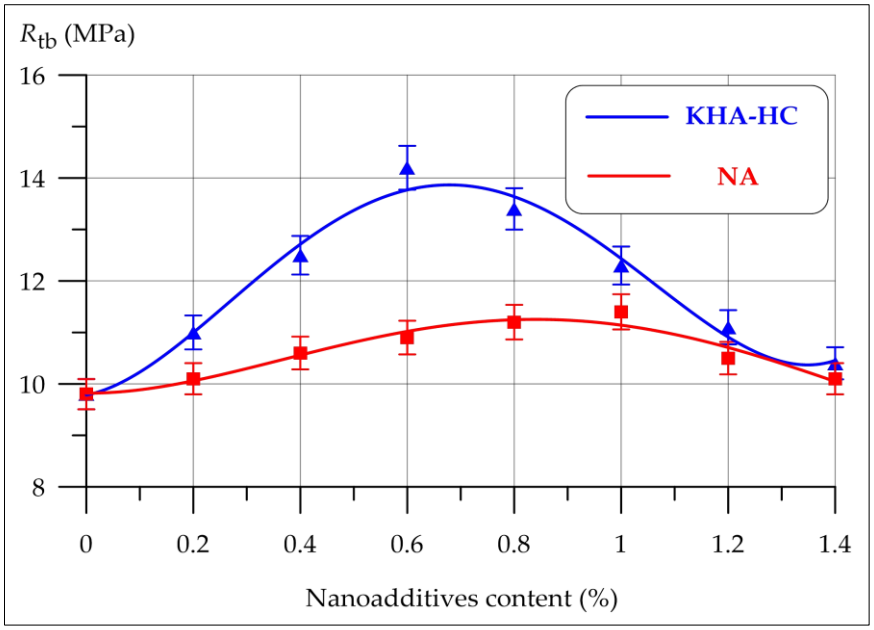

Figure 11. Dependence of the flexural strength (R_{tb}) of HPC on the content of KHA-HC and NA

The compressive strength of HPC can be successfully approximated using a 4^{th} order polynomial with R^2 value depending on the amount of KHA-HC and NA additive (denoted by x in the equation).

$$R_b^{KHA} = 72.83 + 23.46x + 196.9x^2 - 322.1x^3 + 122.5x^4, R^2 = 0.98 \quad (6)$$

$$R_b^{NA} = 73.03 + 5.32x + 39.73x^2 - 46.47x^3 + 11.89x^4, R^2 = 0.95 \quad (7)$$

The high value of the coefficient of determination indicates a functional relationship between the content of nanoadditives and the compressive strength of concrete and can be used by researchers when designing the composition of concrete mixes. The statistical characteristics of trends Equations 6 and 7 (the standard deviation and error table) are presented in Table 8.

Table 8. Standard deviation and errors for the regression equations R_b

Nano filler	σ_e	e_1	e_2	e_3	e_4	e_5	e_6	e_7	e_8
KHA-HC	1.777	-0.100	-0.308	1.832	-3.080	1.360	1.460	-1.268	-1.308
NA	1.011	0.100	-0.268	-0.252	0.733	0.399	-1.787	1.401	-0.356

According to the results presented in Figure 10, it is evident that modification of HPC with nanoadditives had a positive effect on compressive strength. The most significant positive contribution to the performance of HPC was observed in the samples modified with KHA-HC nano-doping. The curve describing the nature of changes in the compressive strength of HPC with different dosages of KHA-HC shows a tendency for strength to increase in the range from 0.2% to 0.6% KHA-HC with a peak value of 107.2 MPa for the KHA-HC/0.6 type composition. The maximum increase in compressive strength was 47.1%. With the increase in the amount of KHA-HC, a decrease in the compressive strength values of HPC was observed. The compressive strength of HPC specimens with KHA-HC/1.4 content increased by 9.9%. Similarly, NA additive also increased the compressive strength. The curve describing the nature of the change in compressive strength of HPC with different dosages of NA illustrates a stable increase in compressive strength in the range from 0.2% to 1.0% NA with the highest strength of 85.3 MPa for the NA/1.0 composition. The highest increase observed in the compressive strength of HPC was recorded as 17.0%. Compositions of the NA/1.2 and NA/1.4 types with higher dosages showed smaller values of increases, which were 9.2% and 5.5%, respectively.

The values of increases characterizing the changes in compressive strength of HPC with nanoadditives depending on their amount are presented in Table 9.

Table 9. Change in compressive strength (ΔR_b) of HPC depending on KHA-HC and NA

Nanoadditive Type	Content (%)							
	0	0.2	0.4	0.6	0.8	1.0	1.2	1.4
	ΔR_b (%)							
KHA-HC	0	14.3	29.5	47.1	39.4	26.6	14.5	9.9
NA	0	3.7	8.5	11.5	14.4	17.0	9.2	5.5

Figure 11 graphically presents the variation of flexural strength (R_{tb}) of HPC according to the amount of KHA-HC and NA additives. The flexural strength of HPC can be successfully approximated using a 4^{th} order polynomial depending on the amount of KHA-HC and NA additives (denoted by x in the equation).

$$R_{tb}^{KHA} = 9.78 + 2.07x + 28.14x^2 - 44.2x^3 + 16.6x^4, R^2 = 0.98 \quad (8)$$

$$R_{b}^{NA} = 9.81 - 0.07x + 8.09x^2 - 9.31x^3 + 2.60x^4, R^2 = 0.94 \quad (9)$$

The statistical characteristics of trends Equations 8 and 9 (the standard deviation and error table) are presented in Table 10.

Table 10. Standard deviation and errors for the regression equations R_{bt}

Nano filler	σ_e	e_1	e_2	e_3	e_4	e_5	e_6	e_7	e_8
KHA-HC	0.240	-0.017	-0.003	0.214	-0.431	0.238	0.134	-0.190	-0.144
NA	0.149	0.020	-0.040	-0.041	0.120	0.047	-0.259	0.207	-0.053

Similarly, as with the compressive strength, the modification of HPC with nanoadditives increased the flexural strength. The highest increases in flexural strength were recorded for HPC modified with KHA-HC, in comparison with similar compositions with NA. According to Figure 8, an increase in the flexural strength of HPC was observed when the amount of KHA-HC additive was in the range of 0.2%-0.6%. The highest value of flexural strength of 14.2 MPa was possessed by the composition of the KHA-HC/0.6 type, where the value of the increase in compressive strength was 44.9%. Starting from 0.8% to 1.4% KHA-HC, the modification efficiency decreased. Flexural strength of KHA-HC/1.4 doped HPC specimens increased by 8.2%. The increase in flexural strength of NA doped HPC specimens was realized in the range of 0.2%-1.0%. The highest flexural strength of 11.4 MPa was obtained in the NA/1.0 composition and this value increased by 16.3%. In addition, the positive effect on flexural strength decreased as the amount of NA admixture increased above 1%, with only a 3.1% increase at the maximum admixture level of 1.4%. The increase values of the changes in the flexural strength of HPC depending on the amount of nano additives are given in Table 11.

Table 11. Change in flexural strength (ΔR_{tb}) of HPC depending on the KHA-HC and NA amount

Nanoadditive Type	Content (%)							
	0	0.2	0.4	0.6	0.8	1.0	1.2	1.4
	ΔR_{tb} (%)							
KHA-HC	0	12.2	27.6	44.9	36.7	25.5	13.3	8.2
NA	0	3.1	8.2	11.2	14.3	16.3	7.1	3.1

Based on the data on the increase in compressive strength and flexural strength presented in Tables 8 and 9, it is evident that modification of HPC with various types of nanoadditives promotes an increase in strength properties. The greatest positive effect, determined by the increase in strength properties, was observed for HPC compositions modified with the KHA-HC additive, compared to HPC compositions modified with the NA additive. The maximum values of increases in compressive and flexural strength were observed for HPC compositions with 0.6% KHA-HC, which amounted to 47.1% and 44.9%, respectively. The HPC composition modified with 1.0% NA had maximum increases in compressive and flexural strength of 17.0% and 16.3%, respectively. The improvement in strength properties when modifying HPC with the addition of colloidal chemically pure nanodiamonds of cavitation synthesis can be interpreted as follows. As established in a previously performed study [50], the increase in the strength properties of concrete with the addition of KHA-HC is associated with the mechanism of interaction of colloidal particles in cement concrete mixtures. Around the nanodiamond particles, clusters of widely dispersed and dense CSN zones form; these structures create an intrinsic self-reinforcing effect in the cement matrix [51, 52].

The accumulation and interweaving of extended CSN zones make the composite structure denser and stronger. The strength increase observed in HPC with up to 1% NA admixture is mainly due to the fact that NA particles promote cement hydration and increase the total amount of hydration products formed. NA particles accelerate the chemical bonding of $Ca(OH)_2$ formed during hydration reactions, resulting in the accelerated formation of CASH, CAH and CSH, which form the future denser and stronger HPC structure. In turn, NA particles that have not entered into the hydration reaction can fill the pores in the HPC structure. At higher dosages, NA particles begin to agglomerate and stick together and cannot fully enter into the hydration reaction and be evenly distributed throughout the composite structure, which explains the decrease in strength properties after the best peak strength values at a dosage of 1% [38, 66, 67].

Furthermore, Figure 12 presents the results of the determination of water absorption values (W) of KHA-HC and NA doped HPC samples.

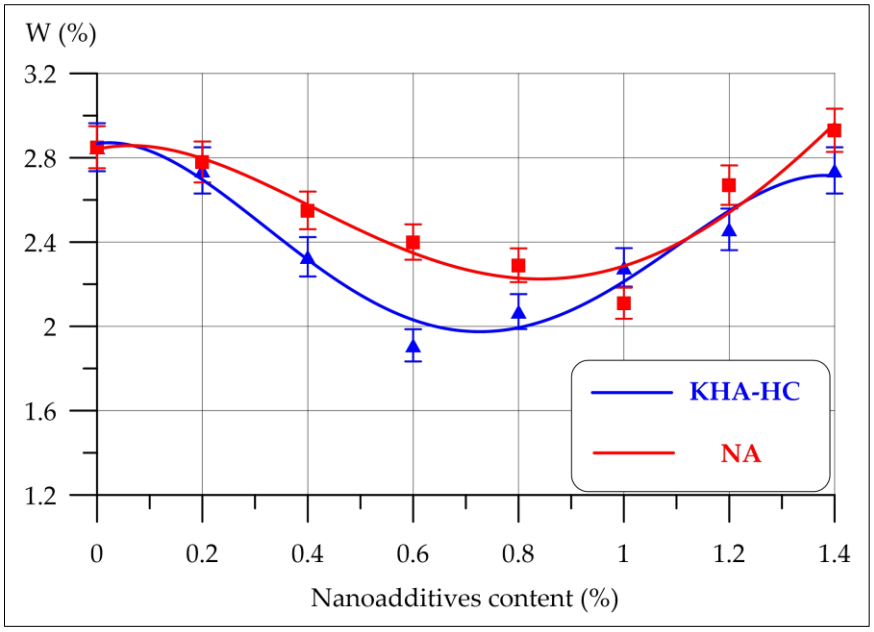

Figure 12. Water absorption (*W*) of HPC versus KHA-HC and NA content

The dependences of water absorption (W) of HPC on KHA-HC and NA (x in equations) content are also well described by a 4th degree polynomial.

$$W^{KHA} = 2.86 + 0.35x - 8.07x^2 + 10.90x^3 - 3.83x^4, R^2 = 0.96 \quad (10)$$

$$W^{NA} = 2.84 + 0.55x - 4.84x^2 + 5.00x^3 - 1.27x^4, R^2 = 0.90 \quad (11)$$

The statistical characteristics of trends Equations 10 and 11 (the standard deviation and error table) are presented in Table 12.

Table 12. Standard deviation and errors for the regression equations *W*

Nano filler	σ_e	e_1	e_2	e_3	e_4	e_5	e_6	e_7	e_8
KHA-HC	0.077	0.017	-0.044	-0.013	0.121	-0.076	-0.067	0.089	-0.026
NA	0.097	-0.009	0.016	0.027	-0.052	-0.061	0.176	-0.129	0.032

According to Figure 12, the curve of change in water absorption values of HPC doped with KHA-HC has the following character: A steady decrease in water absorption was recorded when the amount of KHA-HC was in the range of 0.2%-0.6%. In the KHA-HC/0.6% composition, the minimum water absorption was measured as 1.91%, which is 33.0% lower than the control sample. When the amount of KHA-HC increases in the range of 0.8%-1.4%, the positive effect of modification in HPC decreases. The KHA-HC/1.4 type composition had a water absorption value of 2.74%, which is 3.9% less than the control. The addition of NA led to a decrease in the water absorption capacity of HPC. According to Figure 9, when the amount of NA was in the range of 0.2%-1.0%, the water absorption values of HPC decreased. The minimum water absorption value of HPC at NA/1.0 composition was measured as 2.11%, which is 26.0% lower than the control sample. When the amount of additive was increased thereafter, an inverse change in the water absorption values was observed. The water absorption changes of HPC depending on the amount of nano-additive are given in Table 13.

Table 13. Change in water absorption (Δ*W*) of HPC depending on the amount of KHA-HC and NA

Nanoadditive type	Content (%)							
	0	0.2	0.4	0.6	0.8	1.0	1.2	1.4
	Δ*W* (%)							
KHA-HC	0	–3.9	–18.2	–33.0	–27.4	–20.0	–13.7	–3.9
NA	0	–2.5	–10.5	–15.8	–19.6	–26.0	–6.3	2.8

Reduction of HPC water absorption is a progressive improvement of the overall structure of composites due to modification with nanoadditives. Inclusion of KHA-HC and NA particles in optimal dosages ensures a denser HPC structure due to the operating principle of nanoadditives described above [37, 50].

In conclusion, in the light of the studies on the physical and mechanical properties of HPC modified with nano additives, the following main conclusions were obtained:

Slump of HPC mixtures: According to the research findings, HPC modified with the addition of KHA-HC (chemically pure, cavitation-synthesized nanodiamond) improves the workability (cone spread value) of the mixture. While the cone spread value was 693 mm for the HPC blend with control composition, this value was measured as approximately 750 mm for the blend with maximum 1.4% KHA-HC additive. Modification of HPC with oxide nanoparticles affects 1%, which exclusively increases the cone spread value to 739 mm. Higher content of NA particles provided the opposite effect;

HPC density: KHA-HC and NA additives, when added in the range of 0%-1.4% and in 0.2% increments, did not affect the inverse trend of the curve of the change in density of HPC; the density was measured between 2234-2275 kg/m³ for all experimental compositions;

HPC strength properties: It was determined that KHA-HC additive increased the strength properties of HPC more than NA and the most effective dose was 0.6%, which resulted in 47.1% and 44.9% increase in tensile and flexural strengths, respectively. The best dosage of NA is formed by 1.0% and changed the increase in elongation and bending strength of 17.0% and 16.3%, respectively;

HPC water absorption: The modification of the KHA-HC additive represents a lower water absorption of HPC in relation to HPC compositions with NA. The best dosage of KHA-HC is 0.6% and a decrease in water absorption of 33.0% is introduced. The best dosage of NA is 1.0% and a decrease in water absorption of 26.0% is introduced. Figures 13-15 show the microstructures of the control samples HPC and KHA-HC/0.6 and NA/1.0 and the EDS spectra characterizing the elemental composition of the composites in local areas.

Figure 13 shows the SEM and EDS structures of the control sample HPC.

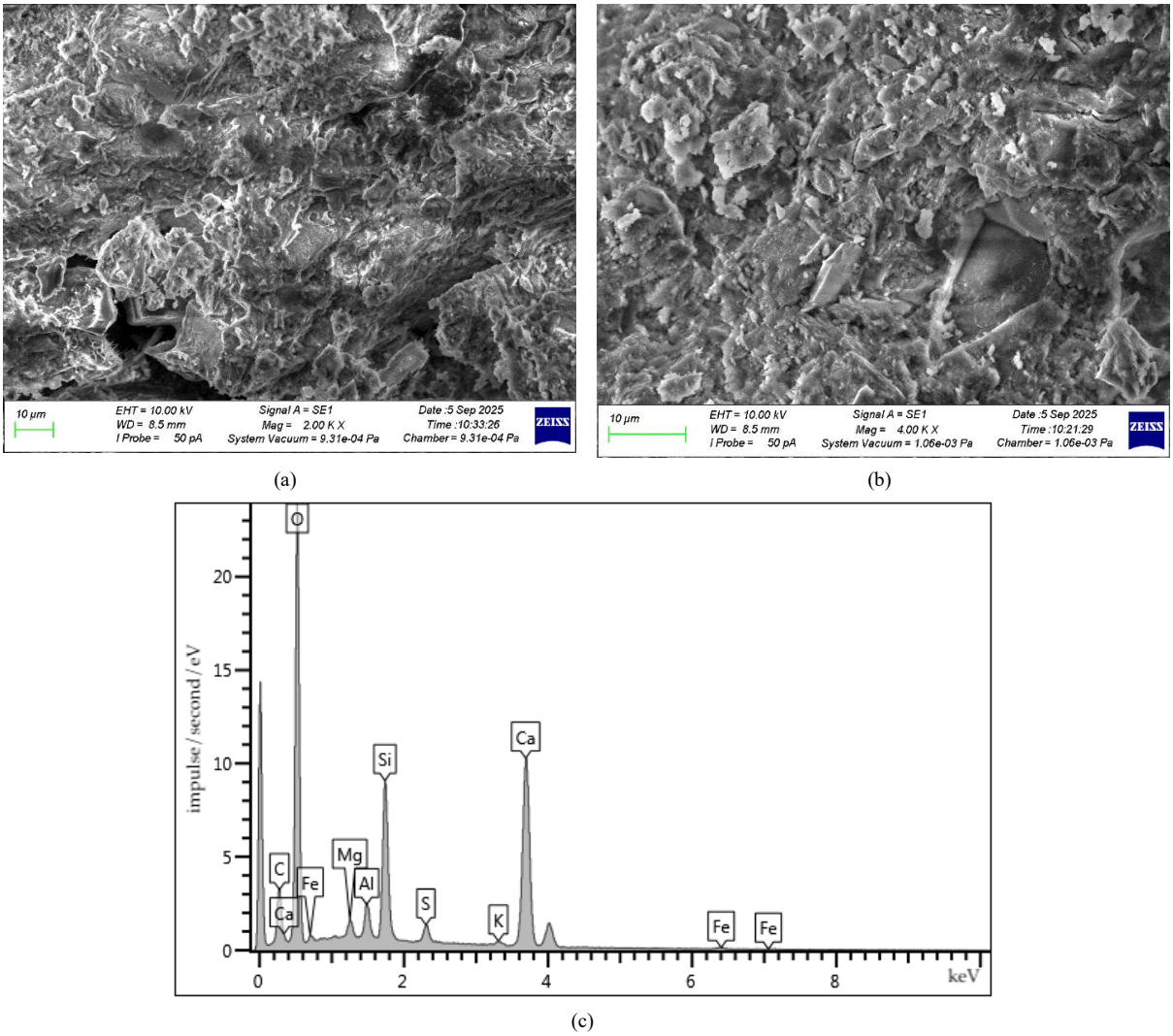

Figure 13. SEM and EDS of the HPC structure of the control composition: (a) with magnification of 2000×; (b) with magnification of 4000×; (c) EDS analysis

The HPC of the control composition has a homogeneous structure. Zones of accumulation of ettringite crystals are observed. As a rule, during the hydration of Portland cement, the formation of ettringite crystals is possible at the very early stage until the hydration of silicate minerals that has begun leads to such an increase in the concentration of $Ca(OH)_2$, at which the growth of ettringite crystals becomes impossible. The smallest particles of ettringite, in the absence of growth conditions, can be preserved for a long time in the cement matrix and are capable of recrystallization when more favorable conditions occur with a decrease in the concentration of Ca^{2+},OH^-,SO_4^{2-} ions in the pore fluid of concrete to certain limits [50, 51]. Recrystallization results in the formation of large ettringite crystals which, accumulating in pores and microcracks, create additional stresses in the composite structure and accelerate the process of its destruction. Accordingly, the presence of clusters of ettringite crystal zones is undesirable. Microcracks and pores were also recorded in the structure of the HPC control composition. According to the results of EDS analysis, a number of chemical elements were identified with the following mass ratio: C (5.22%), O (43.13%), Mg (0.80%), Al (1.67%), Si (8.63%), S (1.35%), K (0.56%), Ca (36.65%), Fe (1.98%).

Figure 14 shows the SEM and EDS structures of the composite of the KHA-HC/0.6 type.

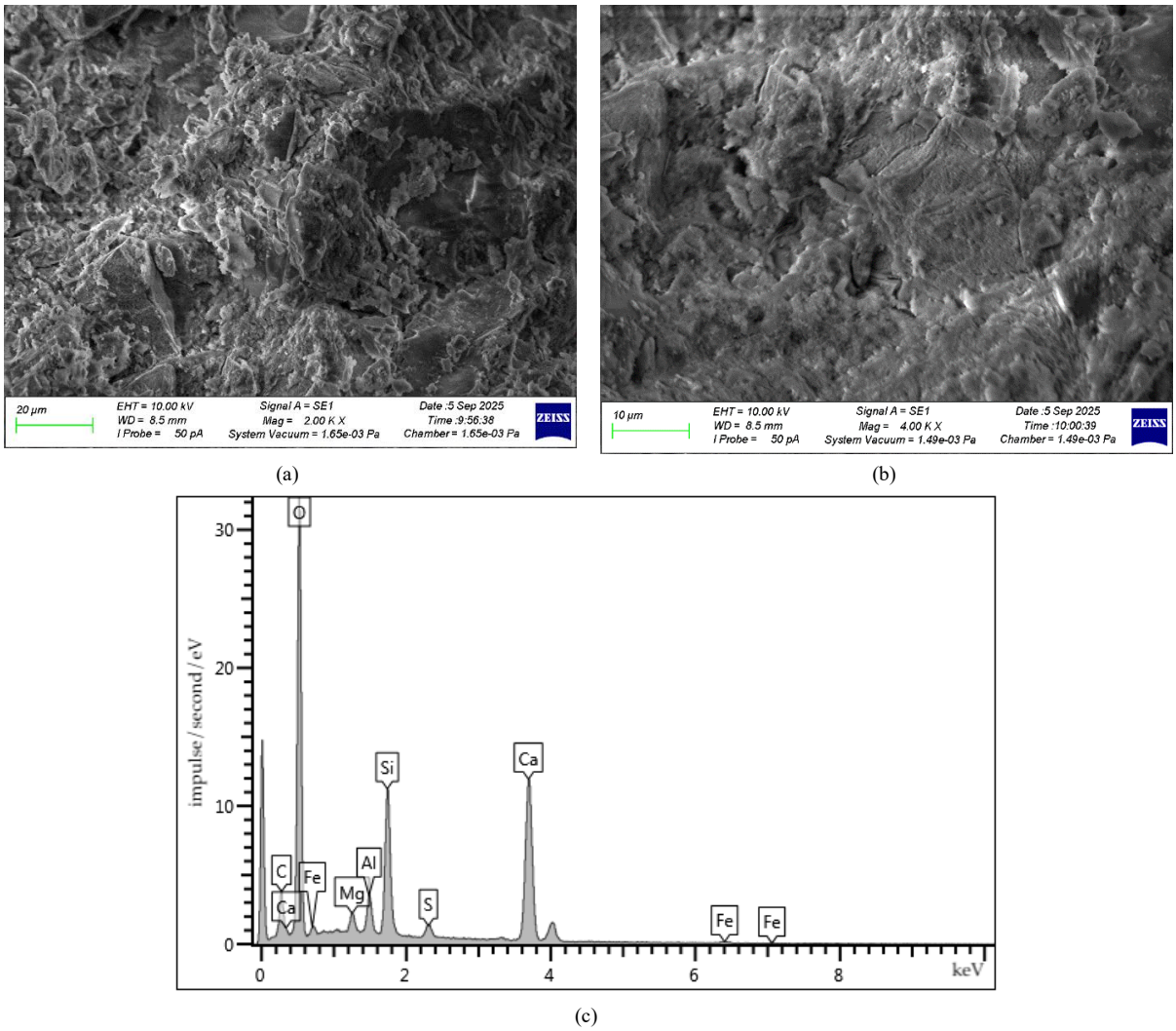

Figure 14. SEM and EDS of the HPC structure of the KHA-HC/0.6 type: (a) with magnification of 2000×; (b) with magnification of 4000×; (c) EDS analysis

The microstructure of the HPC of the KHA-HC/0.6 type is highly uniform and compact. No clusters of ettringite crystal zones were recorded. Multiple zones of accumulation of hydration products are observed - mainly calcium hydrosilicates (CSH). Based on the results of EDS analysis, a number of chemical elements were identified with the following mass ratio: C (3.97%), O (45.53%), Mg (0.99%), Al (2.07%), Si (8.90%), S (1.15%), Ca (35.22%), Fe (2.17%).

Figure 15 shows the SEM and EDS structures of the NA/1.0 type composite.

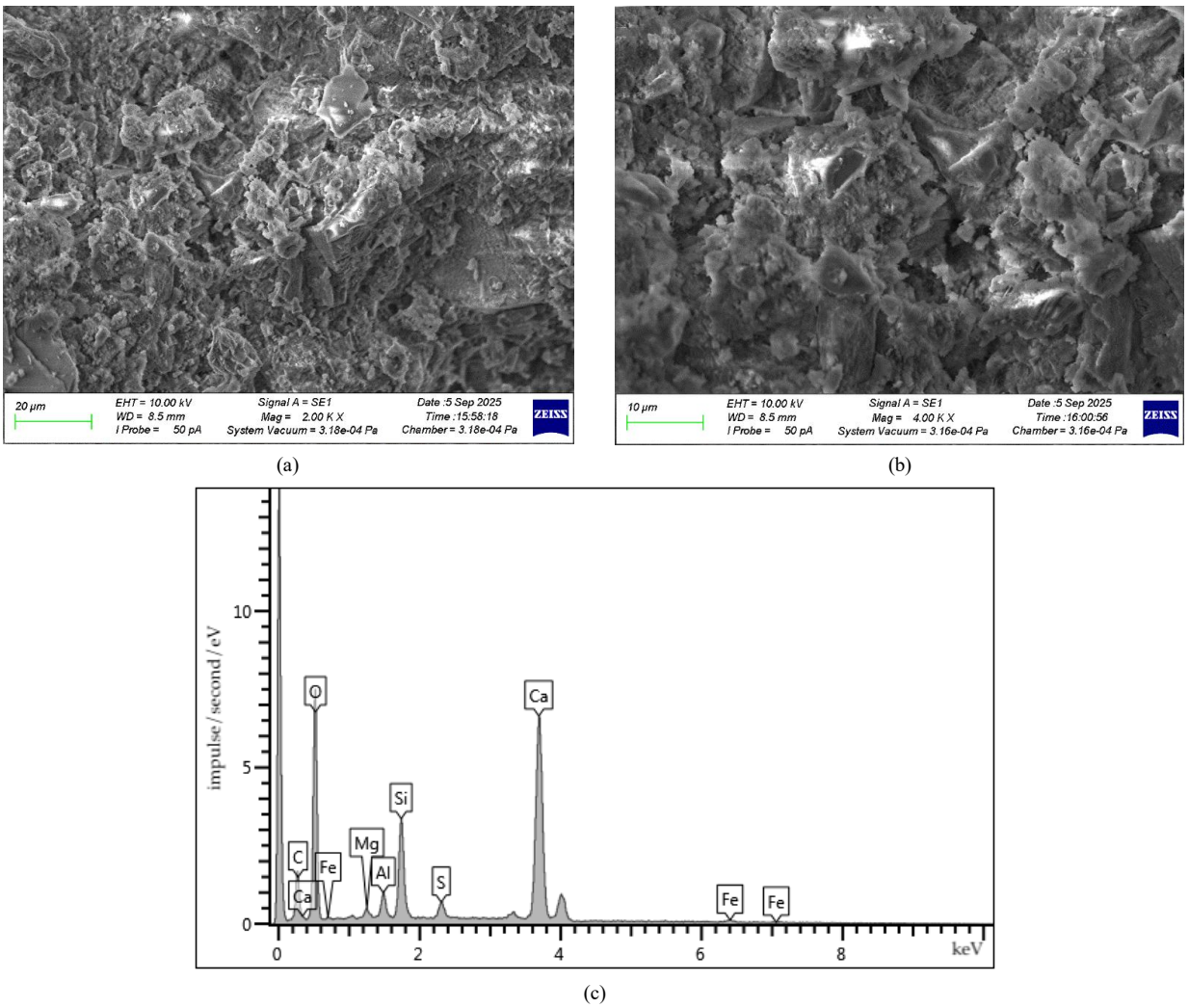

Figure 15. SEM and EDS structures of HPC of NA/1.0 type composition: (a) with magnification of 2000×; (b) with magnification of 4000×; (c) EDS analysis

HPC of NA/1.0 type composition have a homogeneous and compact structure. Single clusters of ettringite crystal zones and multiple zones of CSH clusters are recorded. Microcracks are also observed in the structure of this composite. According to the results of EDS analysis, a number of chemical elements with the following mass ratio were identified: C (4.75%), O (32.47%), Mg (0.48%), Al (1.45%), Si (6.58%), S (1.55%), Ca (48.65%), Fe (4.07%). Based on the results of SEM and EDS analysis of the HPC structure (Figures 13-15), it was found that these composites have a more homogeneous and compact structure compared to the structure of the control HPC composition. No clusters of ettringite crystal zones were recorded in the composition of the **KHA-HC** /0.6 type HPC, and they are present in smaller quantities in the NA/1.0 type composition. The reduction in the number of clusters of ettringite crystal zones in the structure of the developed composites indicates the effectiveness of the applied nanoadditives and their positive effect on the cement hydration processes occurring at early stages.

To evaluate the combined modification with nanoadditives, a HPC composition with 0.6% KHA-HC and 1.0% NA was prepared. The properties of HPC modified using two different nano-additives are given in Table 14.

Table 14. Properties of HPC modified with a combination of nanoadditives

Mixture type	Cone spread (mm)	ρ (kg/m^3)	R_b (MPa)	R_{tb} (MPa)	W (%)
KHA-HC/0.6 + NA/1.0	730	2273	115.3	15.1	1.45

According to the data presented in Table 14, the combined modification of HPC of two calendar nanoadditives KHA-HC and NA caused an increase in the cone spread increment to 5.3%. The density value was 2273 kg/m^3, which is 0.9% higher than the control composition. A significant improvement in strength properties was recorded, the increments for elongation and contour elongation were 58.2% and 54.1%, respectively. Water absorption decreased by 49.1%. Thus, it was found that the complex modification of KHA-HC and NA nanoadditives is more effective in the process of modifying these nanoadditives separately.

Furthermore, Figure 16 shows the results of the SEM and EDS analysis of the structure of HPC samples modified with KHA-HC/0.6 and NA/1.0.

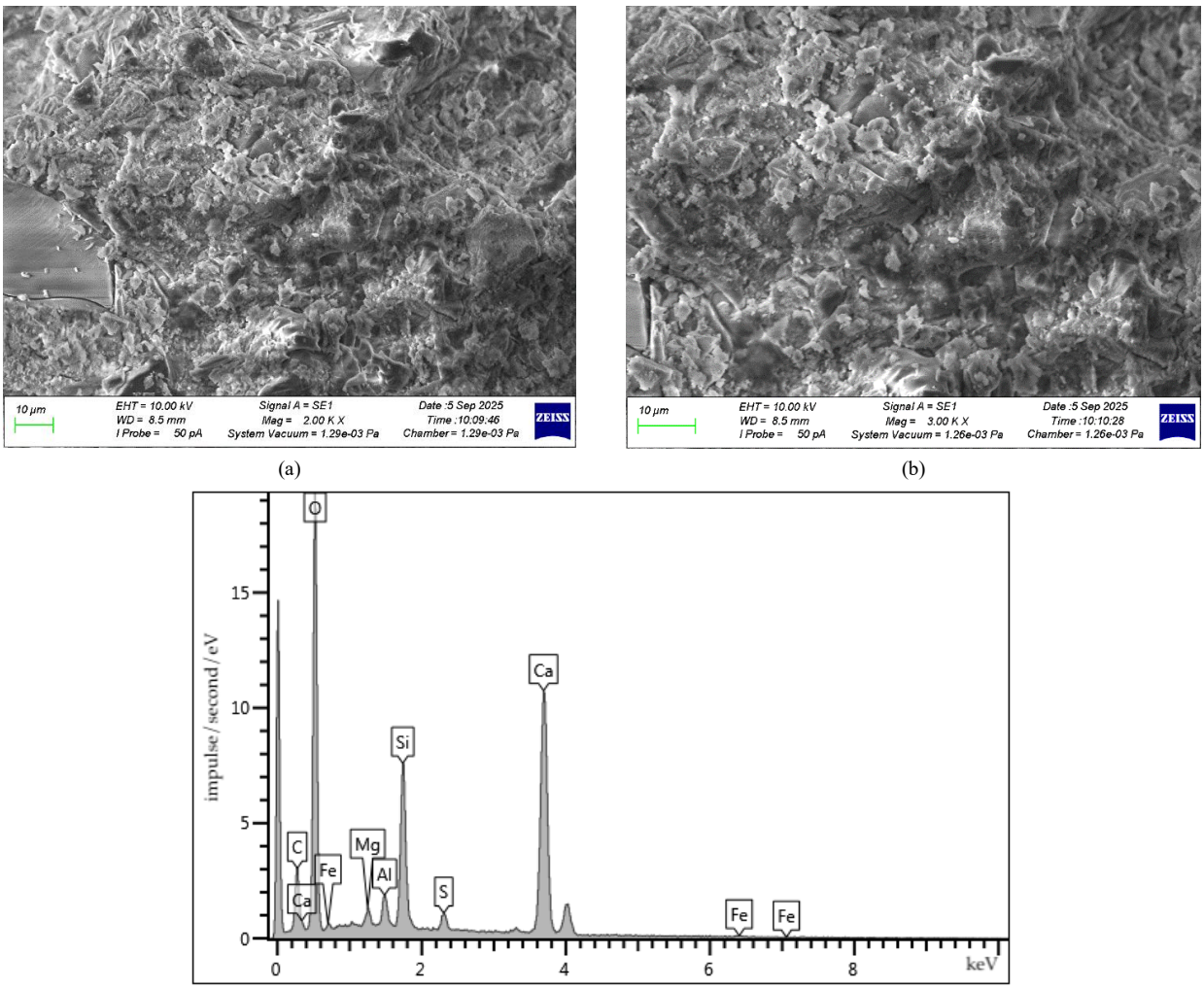

Figure 16. SEM and EDS of the HPC structure of the KHA-HC /0.6 + NA/1.0 type: (a) with magnification of 2000×; (b) with magnification of 4000×; (c) EDS analysis

The microstructure of the HPC of the KHA-HC/0.6 + NA/1.0 type with a combination of two nanoadditives has high homogeneity and compactness and is characterized by a large accumulation of C-S-H zones. Based on the results of the EDS analysis, a number of chemical elements were identified with the following mass ratio: C (4.28%), O (40.64%), Mg (0.69%), Al (1.34%), Si (7.91%), S (1.23%), Ca (42.37%), Fe (1.53%). No clusters of ettringite crystal zones were recorded, which also indicates a positive effect of the combination of these nanoadditives on the hydration processes of Portland cement occurring at early stages. The stages of the hydration process of hardening include the following main stages: dissolution of clinker mineral crystals in water with the formation of supersaturated aqueous solutions; crystallization from solutions of crystal hydrates; recrystallization of crystal hydrates over time with the formation of stable compounds; formation of the structure of the cement matrix [50, 51]. The nanoadditives studied in this study are actively involved in the hydration processes at early stages and ensure an improvement in the future structure and properties of composites. Modification of HPC with two types of nanoadditives, KHA-HC and NA, has a complex effect and ensures a high increase in strength properties. Combining several types of nanoadditives and including them in cement systems to improve mechanical and performance properties is an effective formulation solution and is confirmed by previous studies. Combining 1% nanosilica and nanometakaolin demonstrated an increase in compressive and tensile strength by 14.2% and 7.7%, respectively [68]. The introduction of 2% nano-Al2O3 and nano-TiO2 improves the mechanical properties and durability of concrete [69]. Cement mortars with nanometakaolin and graphene oxide demonstrate significant increases in splitting tensile strength by 71%, compressive strength by 20%, and an improvement in pore structure [70]. Similar results of experimental studies confirming the high efficiency of complex nanomodification are presented in other studies [71-73].

Results of changes in properties of HPC modified using two different nano-additives, KHA-HC and NA, presented above, confirm the effectiveness of their application. The best parameters of HPC modification for each type of nanoadditive were determined. The KHA-HC nanoadditive is introduced into the HPC composition together with part of the mixing water at the final stage of mixing in an amount of 0.6% of the binder weight. NA nano admixture is added to the HPC mix at 1% of the cement weight in dry form and after mixing with the other dry components, the mix water is added. It is worth noting that each of the considered nanoadditives has a different mechanism of interaction with

cement hydration products. Nanomaterials form nanostructures in cement composites, regulating the structure of the cement matrix and reducing its porosity. The working principle of chemically pure, synthesized KHA-HC particles can be summarized as follows: These particles interact with colloidal particles in the concrete mix during the active phase of hydration reactions [50]. The homogeneous distribution and interaction of colloidal particles in the HPC mixture determines its future properties such as density and mechanical strength. Since the forces of dispersed interaction of colloidal particles have a certain electrostatic nature of fields with approximately identical electric field strengths, the inclusion of KHA-HC particles in this process of colloidal interactions of concrete mix particles will cause significant resonant field amplifications near the surface of KHA-HC particles. This, in turn, leads to spatial changes in the processes of formation of the corresponding HPC crystal hydrates.

Accordingly, additional clusters of cement hydration product zones CASH, CAH and CSH with different lengths are formed around KHA-HC particles. The chaotic distribution of extended zones of cement hydration product accumulation around KHA-HC particles in the composite structure has the so-called internal effect of micro-reinforcement of the overall composite structure, which ensures improvement of the structural organization and strength of HPC [49]. Next, we will consider the mechanism of NA particles operation in the structure of cement concrete mixtures. Al2O3 nanoparticles have high surface energy and accelerate the cement hydration process both at the initial and final stages. NA particles are actively involved in the hydration process and are incorporated into the CSH and CASH gel phases. As a result, the hydration products are more evenly distributed and the overall structure of the composite is more regular and organized [37, 74]. Overall, the complex structure-forming and modifying effects of nanoscale KHA-HC and NA particles are the result of the following interrelated mechanisms:

- Increased packing density of HPC particles;
- Nanoscale KHA-HC and NA particles act as additional crystallization centers and accelerate hydration processes;
- Zoning of the hardening structure by nanoscale KHA-HC and NA particles can be accompanied by the formation of a more organized structure of hydrate phases;
- Chemical participation of nanoscale particles in heterogeneous phase formation processes of hydrate compounds [50, 74].

It should be emphasized that results obtained from this study are confirmed and consistent with other similar studies that examined the modification of cement concrete NS и NC (Table 15), with carbon nanoadditives (Table 16) and Al2O3 nanoparticles (Table 17).

Table 15. Effect of NS and NC on the properties of composites

Reference number	Type of nanoadditive	Optimal content	Result obtained
[75]	NS	6.5%	The bond strength between concrete and steel reinforcement increased by 38%.
[76]	NS	4%	A composite with a maximum compressive strength of 22.2 MPa was obtained.
[77]	NS	5%	Increase in Marshall stability by 33.1% and improved rutting resistance
[78]	NC	0.5%	Increase in compressive strength up to 35.5%
[79]	NC	2.5%	Increase in compressive and flexural strength by 25.8% and 19.9%

Table 16. Effects of carbon nano admixtures on physical and mechanical properties of concrete

Reference number	Type of nanoadditive	Optimal content	Result obtained
[80]	Nanocolloidal emulsion of carbon nanotubes	0.3%	Reduced shrinkage during drying. Increase in compressive and flexural strength by 15% and 10%, respectively
[81]	Carbon microfibers/ carbon nanotubes	9 (kg/m^3) / 0.32 (kg/m^3)	Significant improvements in mechanical properties were obtained. Increase in compressive strength by up to 39% and tensile strength by up to 313%
[82]	Carbon nanotubes	0.02%	Increase in compressive strength by 31.5%
[83]		0.2%	Increase in tensile and flexural strength by 50% and 24.4%, respectively
[84]		0.05%	Improved mechanical properties and reduced permeability for chloride ions
[85-88]		0.036– 2%	Composites with improved microstructure, denser and with high mechanical characteristics were obtained
[55]	Nanodiamonds	0.30%	Increase in compressive strength by up to 10%
[89]	Graphene oxide	Water solution for processing fillers with a concentration of 0.5 mg/ml	Reduction in water absorption by 30%. Increase in strength by 32%
[90]		0.05%	Accelerate hydration processes and ensure an increase in strength by 25%
[91]			Reduction in pore size. Increases in compressive strength by 14.61%, flexural strength by 6.09% and elastic modulus by 27.38%
[92]		0.03%	Improving the mechanical properties and wear resistance of ultra-high-strength concrete

Table 17. Results of the effect of NA particles on the properties of concrete

Reference number	Type of nanoadditive	Optimal content	Result obtained
[37, 93]	Al_2O_3 nanoparticles	0.5-1.0%	Improved adhesion of reinforcement to concrete and operational properties of concrete
[94]	Al_2O_3 nanoparticle sol	Processing of fillers	Reduced total porosity of concrete and capillary porosity of cement stone
[95]	Al_2O_3 nanoparticles	3%	Reduced slump of self-compacting concrete mixtures. Reducing composite porosity and increasing compressive strength
[38]	Al_2O_3 nanoparticles	1.0%	Bending strength, compressive strength and elastic modulus were improved by 16.87%, 20.58% and 14.08% respectively

Comparative analysis with the results of studies by other authors confirms the possibility and effectiveness of using carbon nanomaterials (carbon nanotubes, nanodiamonds, graphene oxide) for modifying cement composites, including HPC. It has been established that at relatively low dosages of these nanomaterials 0.03–2% of the mass of the binder component; it is possible to achieve significant improvements in the mechanical properties of composites - an increase in compressive strength up to 10-39%, a decrease in water absorption and an increase in resistance to aggressive environments.

The use of Al_2O_3 nanoparticles for modification of cement concretes is a rational formulation solution and allows achieving significant improvements. NA accelerates cement hydration, promotes the formation of additional hydration products such as CASH, CAH and CSH, reduces total and capillary porosity and thus improves the strength and mechanical performance of concrete [96]. In this study, up to 17% increase in strength properties and up to 26% decrease in water absorption values were observed in HPC modified with Al_2O_3 nanoparticles, and these findings are consistent with other studies in the literature (Table 16). In conclusion, this study reveals the potential of KHA-HC and NA nano-additives in enhancing the physical and mechanical performance of HPC when used both separately and in combination. The developed HPC compositions with nanoadditives can be used in real construction practice, including in critical and unique structures that place high demands on the strength of composite materials. Speaking about the limitations of this study, it is worth noting the poorly studied issue regarding the resistance of HPC with KHA-HC and NA nanoadditives to the effects of aggressive environments saturated with sulfate and chloride ions [97, 98]. However, this shortcoming provides a perspective for future research to study in depth the durability properties of the developed HPC. A series of experimental studies of HPC with KNA-NS and NA nanoadditives is planned. Properties such as water resistance, frost resistance, and resistance to chloride and sulfate ion penetration will be determined, which will subsequently allow for a more accurate assessment of the durability of the HPCs developed in this study.

4. Conclusions

In this study, we studied the rheological properties of HPC mixtures, resistance, tensile and bending strength, water absorption and structural features of HPC modified with two types of nanoadditives - chemically pure nanodiamonds of cavitation synthesis (KHA-HC) and oxide nanoparticles (NA). The main findings of this study are as follows:

- The inclusion of KHA-HC in the composition of HPC mixtures up to 1.4% exclusively increases their spread. The increase in the cone spread value was 8.2%. The inclusion of NA particles up to 1% increases the spread of HPC mixtures, then as the amount of NA increases, a decrease in the spread of the mixture is observed.
- Modification of HPC wallpapers such as nanoadditives in side brackets does not have a significant effect on ceiling composites.
- The addition of 0.6% KHA-HC to the HPC composition includes the maximum values of tensile and flexural strength increases in the range of the control HPC, which were 47.1% and 44.9%, respectively. Water absorption decreased by 33.0%. The optimal range of HPC modification with the KHA-HC nanoadditive is in the range from 0.2% to 1.2%.
- The addition of 1.0% NA to the HPC composition in relation to the control HPC takes into account the maximum values of elongation and flexural strength increase of 17.0% and 16.3%, respectively. Water absorption decreased by 26.0%. The optimal range of HPC modification with the NA nanoadditive was in the range from 0.6% to 1.0%.
- Complex modification of HPC with two calendar nanoadditives in the most rational dosages of 0.6% KHA-HC and 1.0% NA provided an improved effect and, accordingly, the best values of strength properties with increases, elasticity and bending of 58.2% and 54.1%. Water absorption decreased by 49.1%.
- Modification of HPC with KHA-HC and NA nanoadditives in optimal quantities improves the initial structure of composites. The microstructure of HPC modified with nanoadditives is characterized by high homogeneity and compactness, a large accumulation of CSH zones, the absence or a small number of clusters of ettringite crystal zones. In the case of KHA-HC, the microstructure of the constant self-reinforcement effect is improved due to the creation of dense clusters of the CSH zone with a large extent around the nanodiamond particles. NA particles are actively embedded in the gel phase of hydration of the products and ensure their uniform distribution, which makes the final structure more organized.

- According to the results of EDS analysis, the elemental composition of the HPC control composition and compositions modified with various nanoadditives is characterized by the presence of the following main elements: C, O, Mg, Al, Si, S, Ca, Fe. The predominant chemical elements are Ca, O, and Si.
- The use of the developed HPC compositions with nanoadditives is preferable in the application of construction practice, including the construction of responsible and durable buildings and structures that place high demands on the strength of composite materials.
- The limitations of this study are the poor understanding of the resistance of HPC with KHA-HC and NA nanoadditives to future aggressive agents and the availability of nanodiamond additives on the market.
- In future studies, the HPC applied and the other nano-additives used will be investigated in detail, especially including their use in combination with nanodiamond.

5. Declarations

5.1. Author Contributions

Conceptualization, S.A.S., E.M.S., A.C, D.E., and Y.O.Ö.; methodology, S.A.S., E.M.S., and A.N.B.; software, E.M., C.A., and D.E.; validation, C.A., A.C., and A.N.B.; formal analysis, A.C. and A.N.B.; investigation, S.A.S., E.M.S., A.N.B., Y.O.Ö., A.C., D.E., E.M., and C.A.; resources, S.A.S.; data curation, E.M.S., D.E., E.M., and A.C.; writing—original draft preparation, D.E., S.A.S., E.M.S., Y.O.Ö., and A.N.B.; writing—review and editing, S.A.S., E.M.S., Y.O.Ö., and A.N.B.; visualization, S.A.S., E.M.S., and A.N.B.; supervision, Y.O.Ö.; project administration, Y.O.Ö.; funding acquisition Y.O.Ö. All authors have read and agreed to the published version of the manuscript.

5.2. Data Availability Statement

The data presented in this study are available on request from the corresponding author.

5.3. Funding

This study was supported by the grant of the Russian Science Foundation No. 25-79-32007, https://rscf.ru/project/25-79-32007/.

5.4. Acknowledgements

The authors would like to acknowledge the administrations of Don State Technical University and Necmettin Erbakan University for their resources and support.

5.5. Conflicts of Interest

The authors declare no conflict of interest.

6. References

[1] Abdul Sahib, M. Q., Farzam, M., & Sukkar, K. A. (2023). Development and Performance Evaluation of UHPC and HPC Using Eco-Friendly Additions as Substitute Cementitious Materials with Low Cost. Buildings, 13(8), 2078. doi:10.3390/buildings13082078.

[2] Tamov, M. M., Rudenko, O. V., & Salib, M. I. F. (2025). Modeling of Shear Strength of Ultra-High-Performance Concrete Beams Using Statistical Learning Tools. Modern Trends in Construction, Urban and Territorial Planning, 4(2), 7–20. doi:10.23947/2949-1835-2025-4-2-7-20.

[3] Huang, P., Li, Y., Ding, F., Liu, X., Bi, X., & Xu, T. (2025). Real-Time Temperature Effects on Dynamic Impact Mechanical Properties of Hybrid Fiber-Reinforced High-Performance Concrete. Materials, 18(14), 3241. doi:10.3390/ma18143241.

[4] Wang, L., Tian, X., Pan, Y., Wu, D., Xu, S., Wang, H., Tian, X., Xu, Y., Guo, H., & Zou, M. (2025). The Properties of Self-Compacting Ultra-High Performance Concrete with Different Types of Mineral Admixtures. Coatings, 15(5), 591. doi:10.3390/coatings15050591.

[5] Adibinia, A., Dehghan Khalili, H., Mohebbi, M. M., Momeni, M., Moradi, P., Ghouhestani, S., & Poorkarimi, A. (2025). Biomaterial-Assisted Self-Healing for Crack Reduction in High-Performance Centrifugal Concrete Piles. Buildings, 15(7), 1064. doi:10.3390/buildings15071064.

[6] Mailyan, L. R., Stel'makh, S. A., Shcherban', E. M., Zherebtsov, Y. V., & Al-Tulaikhi, M. M. (2021). Research of physicomechanical and design characteristics of vibrated, centrifuged and vibro-centrifuged concretes. Advanced Engineering Research (Rostov-on-Don), 21(1), 5–13. doi:10.23947/2687-1653-2021-21-1-5-13.

[7] Birol, T., & Avcıalp, A. (2025). Impact of Macro-Polypropylene Fiber on the Mechanical Properties of Ultra-High-Performance Concrete. Polymers, 17(9), 1232. doi:10.3390/polym17091232.

[8] Xu, J., Li, Y., Huang, Y., Yuan, G., Cao, Z., Zhang, W., Zheng, H., Zang, Y., Mao, X., & Li, M. (2025). Understanding the Role of Quartz Powder Content and Fineness on the Micro-Structure and Mechanical Performance of UHPC. Buildings, 15(9), 1513. doi:10.3390/buildings15091513.

[9] Zhu, P., Du, S., Heng, P., Zhang, L., Zhang, S., & Wu, Y. (2025). Investigation on Mix Proportions of Ultra-High Performance Concrete with Recycled Powder and Recycled Sand. Buildings, 15(7), 1048. doi:10.3390/buildings15071048.

[10] Puzatova, A. V., Dmitrieva, M. A., Tovpinets, A. O., & Leitsin, V. V. (2024). Study of Structural Defects Evolution in Fine-Grained Concrete Using Computed Tomography Methods. Advanced Engineering Research (Rostov-on-Don), 24(3), 227–237. doi:10.23947/2687-1653-2024-24-3-227-237.

[11] Özkılıç, Y. O., Karalar, M., Aksoylu, C., Beskopylny, A. N., Stel'makh, S. A., Shcherban, E. M., Qaidi, S., Pereira, I. da S. A., Monteiro, S. N., & Azevedo, A. R. G. (2023). Shear performance of reinforced expansive concrete beams utilizing aluminium waste. Journal of Materials Research and Technology, 24, 5433–5448. doi:10.1016/j.jmrt.2023.04.120.

[12] Stel'makh, S. A., Shcherban', E. M., Beskopylny, A. N., Mailyan, L. R., Meskhi, B., Shilov, A. A., Evtushenko, A., Chernil'nik, A., El'shaeva, D., Karalar, M., Özkılıç, Y. O., & Aksoylu, C. (2023). Physical, Mechanical and Structural Characteristics of Sulfur Concrete with Bitumen Modified Sulfur and Fly Ash. Journal of Composites Science, 7(9), 356. doi:10.3390/jcs7090356.

[13] Hamakareem, M., Muhedin, D., Hama Rash, A., Qadir, S., & Khodakarami, L. (2024). Toward Optimizing Coarse Aggregate Types and Sizes in High-strength Concrete. ARO-The Scientific Journal of Koya University, 12(2), 33-43.

[14] Kim, K. M., Lee, S., & Cho, J. Y. (2019). Effect of maximum coarse aggregate size on dynamic compressive strength of high-strength concrete. International Journal of Impact Engineering, 125, 107-116. doi:10.1016/j.ijimpeng.2018.11.003.

[15] Shaaban, M., Edris, W. F., Odah, E., Ezz, M. S., & Al-Sayed, A. A. K. A. (2023). A Green Way of Producing High Strength Concrete Utilizing Recycled Concrete. Civil Engineering Journal (Iran), 9(10), 2467–2485. doi:10.28991/CEJ-2023-09-10-08.

[16] Yang, Q., Yang, Q., Peng, X., Xia, K., & Xu, B. (2025). A Review of the Effects of Nanomaterials on the Properties of Concrete. Buildings, 15(13), 2363. doi:10.3390/buildings15132363.

[17] Mohanty, A., Biswal, D. R., Pradhan, S. K., & Mohanty, M. (2025). Impact of Nanomaterials on the Mechanical Strength and Durability of Pavement Quality Concrete: A Comprehensive Review. Eng, 6(4), 66. doi:10.3390/eng6040066.

[18] Bautista-Gutierrez, K. P., Herrera-May, A. L., Santamaría-López, J. M., Honorato-Moreno, A., & Zamora-Castro, S. A. (2019). Recent progress in nanomaterials for modern concrete infrastructure: Advantages and challenges. Materials, 12(21), 3548. doi:10.3390/ma12213548.

[19] Choi, Y. C. (2025). The Effect of Colloidal Nano-Silica on the Initial Hydration of High-Volume Fly Ash Cement. Materials, 18(12), 2769. doi:10.3390/ma18122769.

[20] Chen, X. F., Zhang, X. C., & Yan, G. H. (2025). Multiscale Investigation of Modified Recycled Aggregate Concrete on Sulfate Attack Resistance. Materials, 18(7), 1450. doi:10.3390/ma18071450.

[21] Zeng, P., Abbas, M. A. A. M., Ran, X., & Li, P. (2025). Impermeability, Strength and Microstructure of Concrete Modified by Nano-Silica and Expansive Agent. Journal of Composites Science, 9(3), 108. doi:10.3390/jcs9030108.

[22] Li, X., Yang, W., Wan, S., Li, S., Shi, Z., & Wu, H. (2025). Effects of SiO2 with Different Particle Sizes on the Self-Repairing Properties of Microbial Mineralized Cement Mortar. Applied Sciences (Switzerland), 15(4), 2098. doi:10.3390/app15042098.

[23] Guan, D., Pan, T., Guo, R., Wei, Y., Qi, R., Fu, C., Zhang, Z., & Zhu, Y. (2024). Fractal and Multifractal Analysis of Microscopic Pore Structure of UHPC Matrix Modified with Nano Silica. Fractal and Fractional, 8(6), 360. doi:10.3390/fractalfract8060360.

[24] Guo, D., Guo, M., Zhou, Y., & Zhu, Z. (2024). Use of nano-silica to improve the performance of LC3-UHPC: Mechanical behavior and microstructural characteristics. Construction and Building Materials, 411, 134280. doi:10.1016/j.conbuildmat.2023.134280.

[25] Ghafari, E., Arezoumandi, M., Costa, H., & Júlio, E. (2015). Influence of nano-silica addition in the durability of UHPC. Construction and Building Materials, 94, 181–188. doi:10.1016/j.conbuildmat.2015.07.009.

[26] Golewski, G. L. (2024). Determination of Fracture Mechanic Parameters of Concretes Based on Cement Matrix Enhanced by Fly Ash and Nano-Silica. Materials, 17(17), 4230. doi:10.3390/ma17174230.

[27] Sridhar, R., Aosai, P., Imjai, T., Setkit, M., Shirkol, A., & Laory, I. (2024). Influence of Nanoparticles and PVA Fibers on Concrete and Mortar on Microstructural and Durability Properties. Fibers, 12(7), 54. doi:10.3390/fib12070054.

[28] Li, S., Chen, Y., Tang, C., Wang, J., Liu, R., & Wang, H. (2022). Experimental and Theoretical Study on Carbonization Coefficient Model of NS/SAP Concrete. Buildings, 12(12), 2227. doi:10.3390/buildings12122227.

[29] Nie, L., Li, X., Li, J., Zhu, B., & Lin, Q. (2022). Analysis of High Performance Concrete Mixed with Nano-Silica in Front of Sulfate Attack. Materials, 15(21), 7614. doi:10.3390/ma15217614.

[30] Poudyal, L., Adhikari, K., & Won, M. (2021). Nano calcium carbonate (Caco3) as a reliable, durable, and environment-friendly alternative to diminishing fly ash. Materials, 14(13), 3729. doi:10.3390/ma14133729.

[31] Poudyal, L., Adhikari, K., & Won, M. (2021). Mechanical and durability properties of Portland limestone cement (PLC) incorporated with nano calcium carbonate (CaCO3). Materials, 14(4), 1–19. doi:10.3390/ma14040905.

[32] Chang, C., Ning, H., Song, M., Ma, Y., Wang, X., Ketekun, B. T., Kawkabi, K. W., & Long, X. (2025). Enhancing mechanical properties of high-strength recycled concrete with basalt fiber and nano-calcium carbonate: Experimental and numerical investigations. Construction and Building Materials, 489, 142264. doi:10.1016/j.conbuildmat.2025.142264.

[33] Shah, H. A., Wang, Y., Banthia, N., & Meng, W. (2025). Enhancing nano-CaCO3 dispersion with cellulose nanocrystals for high-strength low-carbon concrete. Cement and Concrete Composites, 164, 106227. doi:10.1016/j.cemconcomp.2025.106227.

[34] Shen, D., Kang, J., Shao, H., Liu, C., Li, M., & Chen, X. (2023). Cracking failure behavior of high strength concrete containing nano-CaCO3 at early age. Cement and Concrete Composites, 139, 104996. doi:10.1016/j.cemconcomp.2023.104996.

[35] Hosan, A., & Shaikh, F. U. A. (2021). Compressive strength development and durability properties of high volume slag and slag-fly ash blended concretes containing nano-CaCO3. Journal of Materials Research and Technology, 10, 1310–1322. doi:10.1016/j.jmrt.2021.01.001.

[36] Dang, V. P., Noh, H. W., & Kim, D. J. (2024). Effects of combined nanoparticles on dynamic strength of ultra-high-performance fiber-reinforced concrete. Journal of Building Engineering, 96, 110508. doi:10.1016/j.jobe.2024.110508.

[37] Zhang, H., Wang, Z., Zhang, T., & Li, Z. (2024). Foam Stabilization Process for Nano-Al2O3 and Its Effect on Mechanical Properties of Foamed Concrete. Nanomaterials, 14(18), 1516. doi:10.3390/nano14181516.

[38] Chu, H., Wang, Q., Gao, L., Jiang, J., & Wang, F. (2022). An Approach of Producing Ultra-High-Performance Concrete with High Elastic Modulus by Nano-Al2O3: A Preliminary Study. Materials, 15(22), 8118. doi:10.3390/ma15228118.

[39] Moghaddam, H. H., Lotfollahi-Yaghin, M. A., & Maleki, A. (2025). Comprehensive analysis of mechanical characteristics in self-compacting concrete (SCC) with aluminum oxide (Al2O3) nanoparticles and glass fibers: An experimental and analytical investigation. Case Studies in Construction Materials, 22, 4095. doi:10.1016/j.cscm.2024.e04095.

[40] Ahmed, D. N. Y., & Alkhafaji, F. F. (2020). Enhancements and Mechanisms of Nano Alumina (Al2O3) on Wear Resistance and Microstructure Characteristics of Concrete Pavement. IOP Conference Series: Materials Science and Engineering, 871(1), 12001. doi:10.1088/1757-899X/871/1/012001.

[41] Elahi, N., & Zeinalipour-Yazdi, C. D. (2025). Advances in the Synthesis of Carbon Nanomaterials Towards Their Application in Biomedical Engineering and Medicine. C, 11(2), 35. doi:10.3390/c11020035.

[42] Panich, A., Froumin, N., Aleksenskii, A., & Chizhikova, A. (2025). XPS Study of Grafting Paramagnetic Ions onto the Surface of Detonation Nanodiamonds. Nanomaterials, 15(4), 260. doi:10.3390/nano15040260.

[43] Zhou, S., Handschuh-Wang, S., & Wang, T. (2024). Deposition of Diamond Coatings on Ultrathin Microdrills for PCB Board Drilling. Materials, 17(22), 5593. doi:10.3390/ma17225593.

[44] Ding, H., Pan, Z., Loh, Y. M., Wang, C., & Tsoi, J. K. H. (2024). Effects of Nano-Diamond-Coated Milling Bits on Cutting Dental Zirconia. Coatings, 14(4), 473. doi:10.3390/coatings14040473.

[45] Zhuang, S., Cao, Y., Song, W., Zhang, P., & Choi, S. B. (2024). Effect of Additives on Tribological Performance of Magnetorheological Fluids. Micromachines, 15(2), 270. doi:10.3390/mi15020270.

[46] Lu, T., Chen, Y., Sun, M., Chen, Y., Tu, W., Zhou, Y., Li, X., & Hu, T. (2025). Multifunctional Carbon-Based Nanocomposite Hydrogels for Wound Healing and Health Management. Gels, 11(5), 345. doi:10.3390/gels11050345.

[47] Esen, M., Yilmaz, A. C., & Kavak, H. (2025). Structural and Tribological Analysis of Multilayer Carbon-Based Nanostructures Deposited via Modified Electron Cyclotron Resonance–Chemical Vapor Deposition. Applied Sciences (Switzerland), 15(6), 3402. doi:10.3390/app15063402.

[48] Piya, A. K., Yang, L., Emami, N., & Morina, A. (2025). Effect of Nanodiamonds on Friction Reduction Performance in Presence of Organic and Inorganic Friction Modifiers. Lubricants, 13(1), 1. doi:10.3390/lubricants13010001.

[49] Speranza, G. (2021). Carbon nanomaterials: Synthesis, functionalization and sensing applications. Nanomaterials, 11(4), 967. doi:10.3390/nano11040967.

[50] Beskopylny, A. N., Stel'makh, S. A., Shcherban', E. M., Varavka, V., Meskhi, B., Mailyan, L. R., Kovtun, M., Kurlovich, S., El'shaeva, D., Chernil'nik, A., & Drogan, E. (2024). Performance and mechanism of the structure formation and physical-mechanical properties of concrete by modification with nanodiamonds. Construction and Building Materials, 452, 138994. doi:10.1016/j.conbuildmat.2024.138994.

[51] Gupta, N., Wang, Q., Wen, G., & Su, D. (2017). Nanodiamonds for catalytic reactions. Nanodiamonds, 439–463. doi:10.1016/B978-0-32-343029-6.00019-2.

[52] Tevyashev, A., & Shitikov, E. (2009). On the possibility of controlling the properties of cement concrete using nanomodifiers. Eastern-European Journal of Enterprise Technologies, 4(7), 35-40.

[53] Zhang, Y., Qin, Y., Guo, Z., & Li, D. (2023). Research on Performance Deterioration of Multi-Walled Carbon Nanotube–Lithium Slag Concrete under the Coupling Effect of Sulfate Attack and Dry–Wet Cycles. Materials, 16(14), 5130. doi:10.3390/ma16145130.

[54] Huang, J., Wang, Z., Li, G., & Yu, J. (2025). Synergistic effects of carbon nanotubes and polyvinyl alcohol on enhancing mechanical strength and carbonation resistance of concrete. Construction and Building Materials, 492, 143036. doi:10.1016/j.conbuildmat.2025.143036.

[55] Chousidis, N., & Zeris, C. (2025). Carbon nanotube reinforcement for cementitious Composites: Advancing thermal stability, mechanical strength and durability in fire-resistant concrete. Journal of Building Engineering, 111, 113587. doi:10.1016/j.jobe.2025.113587.

[56] Reis, E. D., Gatuingt, F., Poggiali, F. S. J., & Bezerra, A. C. S. (2025). Optimizing concrete performance: Influence of carbon nanotubes dispersion techniques. Procedia Structural Integrity, 67, 39–46. doi:10.1016/j.prostr.2025.06.006.

[57] Zhang, X., Luo, T., Zhong, X., Zhou, Y., Peng, X., & Zhao, C. (2025). High-performance foam concrete containing multi-wall carbon nanotubes and ssDNA. Construction and Building Materials, 458, 139523. doi:10.1016/j.conbuildmat.2024.139523.

[58] Zhao, Z., Hu, Y., Zhao, Z., Liu, Y., Xie, C., & Hu, Z. (2025). Effect of curing temperature on the hydration process of carbon nanotubes modified face slab concrete at the ultra-early age. Materials Letters, 394, 138633. doi:10.1016/j.matlet.2025.138633.

[59] Madenci, E., Özkılıç, Y. O., Bahrami, A., Hakeem, I. Y., Aksoylu, C., Asyraf, M. R. M., Beskopylny, A. N., Stel'makh, S. A., Shcherban', E. M., & Fayed, S. (2023). Behavior of functionally graded carbon nanotube reinforced composite sandwich beams with pultruded GFRP core under bending effect. Frontiers in Materials, 10, 1236266. doi:10.3389/fmats.2023.1236266.

[60] GOST R 59715-2022. (2022). Self-compacting fresh concrete. Test Methods. Standartinform, Moscow, Russia. (In Russian).

[61] EN 12390-7:2019. (2019). Testing hardened concrete—Part 7: Density of Hardened Concrete. European Committee for Standardization (CEN), Brussels, Belgium.

[62] GOST R 58277-2018. (2018). Dry building mixes based on cement binder. Test methods. Standartinform, Moscow, Russia.

[63] GOST 12730.3-2020. (2022). Concretes. Method of determination of water absorption. Standartinform, Moscow, Russia.

[64] BS 1881-122:2011+A1:2020. (2020). Testing concrete - Method for determination of water absorption. British Standards Institution (BSI), London, United Kingdom.

[65] Nesvetaev, G. V., Koryanova, Y. I., & Shut, V. V. (2025). Autogenous Shrinkage of Concretes from Highly Mobile and Self-Compacting Mixtures. Modern Trends in Construction, Urban and Territorial Planning, 4(1), 41–53. doi:10.23947/2949-1835-2025-4-1-41-53.

[66] Beskopylny, A. N., Stel'makh, S. A., Shcherban', E. M., Varavka, V., Meskhi, B., Mailyan, L. R., Kovtun, M., Kurlovich, S., El'shaeva, D., & Chernil'nik, A. (2024). Study of the Structure and Properties of Concrete Modified with Nanofibrils and Nanospheres. Buildings, 14(11), 3476. doi:10.3390/buildings14113476.

[67] Beskopylny, A. N., Shcherban', E. M., Stel'makh, S. A., Mailyan, L. R., Meskhi, B., Evtushenko, A., Varavka, V., & Beskopylny, N. (2022). Nano-Modified Vibrocentrifuged Concrete with Granulated Blast Slag: The Relationship between Mechanical Properties and Micro-Structural Analysis. Materials, 15(12), 4254. doi:10.3390/ma15124254.

[68] Abouelnour, M. A., Fathy, I. N., Mahmoud, A. A., Alturki, M., Abdelaziz, M. M., Mostafa, S. A., Mahmoud, K. A., Dahish, H. A., Nabil, I. M., & Fattouh, M. S. (2025). Valorization of nano additives effects on the physical, mechanical and radiation shielding properties of high strength concrete. Scientific Reports, 15(1), 14440. doi:10.1038/s41598-025-99126-1.

[69] Srivastava, A., Mishra, A., & Singh, S. K. (2025). An effect of nano alumina and nano titanium di oxide with polypropylene fiber on the concrete: mechanical and durability study. Discover Civil Engineering, 2(1), 6. doi:10.1007/s44290-025-00161-8.

[70] Mokhtar, M. M. (2024). Evaluating the physico-mechanical performance of cement mortar reinforced with metakaolin/graphene oxide dual nano-additives. Innovative Infrastructure Solutions, 9(3), 75. doi:10.1007/s41062-024-01383-y.

[71] Chaturvedy, G. K., Pandey, U. K., & Mohan, G. (2025). Impact of nano-silica and multi-walled carbon nanotubes on the fire resistance performance of rubberized concrete. Journal of Building Pathology and Rehabilitation, 10(2), 161. doi:10.1007/s41024-025-00668-8.

[72] Das, D. K., & Tiwary, A. K. (2024). Influence of nano bentonite clay and nano fly ash on the mechanical and durability properties of concrete. Clean Technologies and Environmental Policy, 26(11), 3881–3894. doi:10.1007/S10098-023-02610-3.

[73] Yang, X., Yu, K., Li, K., Wang, Z., Ji, F., & Li, M. (2024). Research on mechanical properties of concrete by nano-TiC-BF-fly ash. Scientific Reports, 14(1), 4800. doi:10.1038/s41598-024-55553-0.

[74] Mousavi, S. S., Ahmadi, K., Dehestani, M., & Yeon, J. H. (2025). Influence of Coated Steel Fibers on Mechanical Properties of UHPC Considering Graphene Oxide, Nano-Aluminum Oxide, and Nano-Calcium Carbonate. Fibers, 13(4), 37. doi:10.3390/fib13040037.

[75] Amini Pishro, A., & Feng, X. (2018). Experimental Study on Bond Stress between Ultra High Performance Concrete and Steel Reinforcement. Civil Engineering Journal, 3(12), 1235–1246. doi:10.28991/cej-030953.

[76] Rahmawati, C., Aisyah, S., Sanusi, Iqbal, Maulana, M. M., Erdiwansyah, & Ahmad, J. (2024). Artificial Intelligence Models for Predicting the Compressive Strength of Geopolymer Cements. Civil Engineering Journal (Iran), 10, 37–50. doi:10.28991/CEJ-SP2024-010-03.

[77] Taher, Z. K., & Ismael, M. Q. (2023). Rutting Prediction of Hot Mix Asphalt Mixtures Modified by Nano Silica and Subjected to Aging Process. Civil Engineering Journal (Iran), 9, 1–14. doi:10.28991/CEJ-SP2023-09-01.

[78] Wen, Y., Wang, Z., Yuan, X., & Yang, X. (2025). Optimization of Mechanical Properties and Durability of Steel Fiber-Reinforced Concrete by Nano CaCO3 and Nano TiC to Improve Material Sustainability. Sustainability (Switzerland), 17(2), 641. doi:10.3390/su17020641.

[79] Cui, K., Lau, D., Zhang, Y., & Chang, J. (2021). Mechanical properties and mechanism of nano-CaCO3 enhanced sulphoaluminate cement-based reactive powder concrete. Construction and Building Materials, 309, 125099. doi:10.1016/j.conbuildmat.2021.125099.

[80] Lu, S., Zuo, T., Wang, Z., & Yan, S. (2025). Effects of CNTs/PVA on Concrete Performance: Strength, Drying Shrinkage, and Microstructure. Materials, 18(11), 2535. doi:10.3390/ma18112535.

[81] Martínez, J. D. R., Ríos, J. D., Cifuentes, H., & Leiva, C. (2025). Multi-Scale Toughening of UHPC: Synergistic Effects of Carbon Microfibers and Nanotubes. Fibers, 13(4), 49. doi:10.3390/fib13040049.

[82] Cea, E. J. C., Omisol, C. J. M., Tuble, K. A. Q., Bongabong, A. G., Aguinid, B. J. M., Asequia, D. M. A., Erjeno, D. J. D., Ahalajal, M. A. N., Maravillas, F. P., Cavero, A. I., Dumancas, G. G., Malaluan, R. M., & Lubguban, A. A. (2025). Combined Effect of Multi-Walled Carbon Nanotubes and Silica Fume on Mechanical, Physicochemical, and Thermal Properties of Concrete Composites. Buildings, 15(7), 1087. doi:10.3390/buildings15071087.

[83] Choi, S. J., Lee, J. I., Kim, C. Y., Yoon, J. H., & Kim, K. H. (2024). Effect of Amorphous Metallic Fibers on Thermal and Mechanical Properties of Lightweight Aggregate Cement Mortars Containing Carbon Nanotubes. Materials, 17(22), 5449. doi:10.3390/ma17225449.

[84] Rafieizonooz, M., Kim, J. H. J., Kim, J. S., & Jo, J. Bin. (2024). Effect of Carbon Nanotubes on Chloride Diffusion, Strength, and Microstructure of Ultra-High Performance Concrete. Materials, 17(12), 2851. doi:10.3390/ma17122851.

[85] Kostrzanowska-Siedlarz, A., Musioł, K., Ponikiewski, T., Janas, D., & Kampik, M. (2024). Facile Incorporation of Carbon Nanotubes into the Concrete Matrix Using Lignosulfonate Surfactants. Materials, 17(20), 4972. doi:10.3390/ma17204972.

[86] Lee, D., Lee, S. C., Kwon, O. S., & Yoo, S. W. (2024). Shear Behavior of High-Strength and Lightweight Cementitious Composites Containing Hollow Glass Microspheres and Carbon Nanotubes. Buildings, 14(9), 2824. doi:10.3390/buildings14092824.

[87] Shi, C., Jin, S., Wang, C., & Yang, Y. (2024). Enhancing Flexural Behavior of Reinforced Concrete Beams Strengthened with Basalt Fiber-Reinforced Polymer Sheets Using Carbon Nanotube-Modified Epoxy. Materials, 17(13), 3250. doi:10.3390/ma17133250.

[88] Wu, H., Liu, X., Ma, X., & Liu, G. (2024). Effects of Multi-Walled Carbon Nanotubes and Recycled Fine Aggregates on the Multi-Generational Cycle Properties of Reactive Powder Concrete. Sustainability (Switzerland), 16(5), 2084. doi:10.3390/su16052084.

[89] Antolín-Rodríguez, A., Juan-Valdés, A., Guerra-Romero, M. I., Morán-del Pozo, J. M., Krzywon, R., Maravelaki, P. N., & García-González, J. (2025). Mechanical Performance of Concrete with Graphene-Oxide-Treated Recycled Coarse Ceramic Aggregates: Effects on Aggregate Water Absorption and Workability. Ceramics, 8(3), 104. doi:10.3390/ceramics8030104.

[90] Ginigaddara, T., Devapura, P., Vimonsatit, V., Booy, M., Mendis, P., & Satsangi, R. (2025). A Comprehensive Study of the Macro-Scale Performance of Graphene Oxide Enhanced Low Carbon Concrete. Construction Materials, 5(3), 47. doi:10.3390/constrmater5030047.

[91] Benavente, C., Romero, A., Napa, J., Sanabria, A., Landivar, Y., La Borda, L., Pezo, P., Muñiz, A., & Muñiz, M. (2025). The Influence of Graphene Oxide on the Performance of Concrete: A Quantitative Analysis of Mechanical and Microstructural Properties. Buildings, 15(7), 1082. doi:10.3390/buildings15071082.

[92] He, T., Xie, W., Wang, F., Yu, Z., Xu, F., Li, J., Deng, Y., Ding, Q., Hao, Y., Xu, W., & Yu, H. (2024). A Study on the Mechanism by Which Graphene Oxide Affects the Macroscopic Properties and Microstructure of Abrasion-Resistant Ultra-High-Performance Concrete (UHPC). Coatings, 14(12), 1482. doi:10.3390/coatings14121482.

[93] Li, Y., & Zhang, H. (2025). Enhancing adhesion behaviour of steel and CFRP rebars in Al_2O_3 nanoparticle-reinforced concrete: insights from experimental and finite element analyses. Australian Journal of Structural Engineering, 1–14. doi:10.1080/13287982.2025.2520041.

[94] Muñoz, J. F., Yao, Y., Youtcheff, J., & Arnold, T. (2014). Mixtures of silicon and aluminum oxides to optimize the performance of nanoporous thin films in concrete. Cement and Concrete Composites, 48, 140–149. doi:10.1016/j.cemconcomp.2013.11.013.

[95] Joshaghani, A., Balapour, M., Mashhadian, M., & Ozbakkaloglu, T. (2020). Effects of nano-TiO2, nano-Al2O3, and nano-Fe2O3 on rheology, mechanical and durability properties of self-consolidating concrete (SCC): An experimental study. Construction and Building Materials, 245, 118444. doi:10.1016/j.conbuildmat.2020.118444.

[96] Shcherban, E. M., Stel'makh, S. A., Mailyan, L. R., Beskopylny, A. N., Smolyanichenko, A. S., Chernil'nik, A. A., Elshaeva, D. M., & Beskopylny, N. A. (2024). Structure and Properties of Variatropic Concrete Combined Modified with Nano-and Micro-silica. Construction Materials and Products, 7(2), 3. doi:10.58224/2618-7183-2024-7-2-3.

[97] Turina, V. S., Chepurnenko, A. S., & Akopyan, V. F. (2024). Methodology for determining true temperature stresses during the construction of massive monolithic reinforced concrete structures. Construction Materials and Products, 7(3), 5. doi:10.58224/2618-7183-2024-7-3-5.

[98] Xavier, V. H. C., Salles, A. M. da S. L. de M., Meneghetti, E. M., Maeda, G. H. H., Sousa, A. M. D. de, Félix, E. F., & Prado, L. P. (2025). Experimental and Numerical Analyses on the Flexural Tensile Strength of Ultra-High-Performance Concrete Prisms with and Without Rice Husk Ash. Buildings, 15(10), 1635. doi:10.3390/buildings15101635.